

# Multi-Task Label Discovery via Hierarchical Task Tokens for Partially Annotated Dense Predictions

Jingdong Zhang<sup>\*</sup> · Hanrong Ye · Xin Li · Wenping Wang · Dan Xu

Received: date / Accepted: date

**Abstract** In recent years, simultaneous learning of multiple dense prediction tasks with partially annotated label data has emerged as an important research area. Previous works primarily focus on constructing cross-task consistency or conducting adversarial training to regularize cross-task predictions, which achieve promising performance improvements, while still suffering from the lack of direct pixel-wise supervision for multi-task dense predictions. To tackle this challenge, we propose a novel approach to optimize a set of learnable hierarchical task tokens, including global and fine-grained ones, to discover consistent pixel-wise supervision signals in both feature and prediction levels. Specifically, the global task tokens are designed for effective cross-task feature interactions in a global context. Then, a group of fine-grained task-specific spatial tokens for each task is learned from the corresponding global task tokens. It is embedded to have dense interactions with each task-specific feature map. The learned global and local fine-grained task tokens are further used to discover pseudo task-specific dense labels at different levels of granularity, and they can be utilized to directly supervise the learning of the multi-task dense prediction framework. Extensive experimental results on challenging NYUD-v2, Cityscapes, and PASCAL Context datasets demonstrate significant improvements over existing state-of-the-art methods for partially annotated multi-task dense prediction.

**Keywords** Multi-task Partially Annotated Dense Prediction · Multi-task Learning · Label Discovery

## 1 Introduction

With the rapid development of supervised learning with deep neural networks, various pixel-wise dense prediction tasks with highly complementary properties such as semantic segmentation and depth estimation have achieved great success in multi-task learning (MTL) in recent years [25, 32, 35, 37, 46]. Researchers pursue the learning of them simultaneously in a unified framework, which can effectively model cross-task correlations and achieve superior results in terms of model training costs and performances.

However, in real-world scenarios, obtaining pixel-level annotations is prohibitively expensive, especially when dealing with a set of distinct dense prediction tasks. Each image has to be annotated with pixel labels for all the tasks. Thus, existing works have delved into the problem of multi-task learning with only partially annotated dense labels [17, 22, 33, 42, 44]. Specifically, as illustrated in Fig. 1 (a), given an input image, for  $T$  dense prediction tasks, the task labels are provided for at least one task and at most  $T - 1$  tasks. Learning a multi-task model under this setting is particularly challenging since every input image lacks some of the task supervision signals, and the performance typically drops significantly if compared to the same model trained with full task label supervisions [17].

Directly discovering pseudo task labels in prediction spaces can alleviate this problem to a certain extent, however, it still suffers from the following two severe limitations: (i) Simply discovering labels in prediction spaces cannot take advantage of the abundant task rep-

---

Jingdong Zhang · Xin Li · Wenping Wang  
Department of Computer Science & Engineering, Texas A&M University, College Station, USA  
E-mail: jdzhang@tamu.edu

Hanrong Ye · Dan Xu  
Department of Computer Science and Engineering, Hong Kong University of Sciences and Technology, China

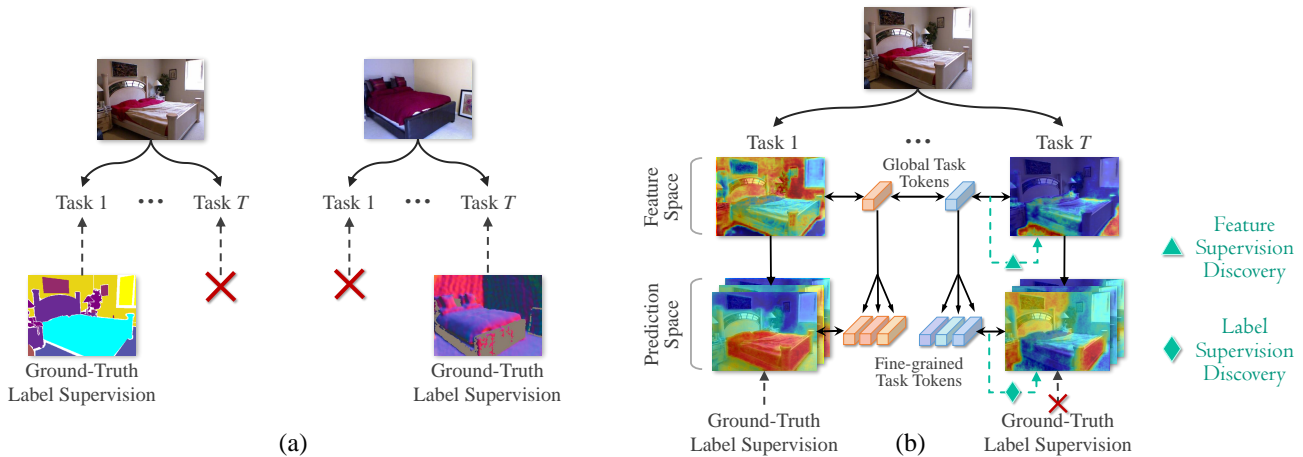


**Fig. 1** (a) Illustration of partially annotated multi-task dense prediction setting. Each input image only has partial task labels from all the tasks. (b) Illustration of the learning of Hierarchical Task Tokens, including global task tokens and fine-grained task tokens, by conducting feature-token interactions in feature and prediction spaces separately. The well-learned hierarchical task tokens can achieve both feature supervision discovery and task label discovery.

representations in feature space. For each specific task, labeled and unlabeled images share all of the network parameters during training, and the distributions of their features and predictions should be consistent. For all dense prediction tasks, rich task-generic representations remain in feature space since the backbone parameter sharing, which are beneficial for building cross-task relations and regularizing unsupervised tasks. In this case, excavating labels only in the prediction spaces fails to exploit consistent representations from different levels among different tasks. (ii) Directly cross-task regularizing the prediction space is difficult and expensive. Since representations in the prediction space are highly semantic on each task, additional heavy mapping networks are required to project the different task predictions into a common space to utilize task correlations for learning regularization [17] between labeled and unlabeled tasks. Therefore, it is critically important to involve the intermediate task features for the task label discovery and regularization.

To effectively tackle the aforementioned challenges, we propose a novel approach that performs task label discovery from both the feature and prediction spaces via an effective design of learnable Hierarchical Task Tokens (HiTTs). HiTTs are sets of compact parameters that are learned in a hierarchical manner to model global inter-task relationships and local fine-grained intra-task relationships, which allows for discovering pixel-wise task pseudo labels straightforwardly based on the modeled correlations with the task tokens.

More specifically, as depicted in Fig. 1 (b), we apply HiTTs during the multi-task decoding stage and jointly optimize them with the multi-task learning network. The HiTTs consists of two hierarchies. The first

hierarchy is a set of global task tokens. The global task tokens are randomly initialized and can perform cross-task feature-token interactions with different task feature maps based on self-attention. These learned task tokens can be used to discover feature-level pseudo supervision by selecting highly activated pixel features correlated to each task. The second hierarchy is the fine-grained task tokens. These tokens are directly derived from the global task tokens with learnable projection layers. They are generated to be spatial token maps to perform interactions within each task-specific feature map at a finer granularity. As the fine-grained task tokens can learn pixel-to-pixel correlation with each task feature map, it thus can help us to discover dense spatial labels for each task. We learn both hierarchies simultaneously in an end-to-end manner, and exploit both levels of supervision signals discovered from the two task-token hierarchies, for optimizing multi-task dense predictions with partially annotated datasets.

In summary, the contribution of this work is three-fold:

- We propose a novel design of Hierarchical Task Tokens (HiTTs), which can learn hierarchical multi-task representations and correlations with only partially annotated training data.
- We exploit the hierarchical task tokens to effectively develop multi-task label discovery strategies and obtain direct multi-task supervision signals from both the feature and the prediction levels.
- Our proposed method significantly outperforms existing state-of-the-art competitors on multi-task partially annotated benchmarks, including NYUD-v2, Cityscapes and PASCAL-Context, and demonstrates

clear effectiveness on challenging dense prediction tasks with limited annotations, including segmentation, depth estimation, normal estimation and edge detection, etc.

## 2 Related Work

**Multi-task Dense Prediction.** Dense prediction tasks aim to produce pixel-wise predictions for each image. Common tasks including semantic segmentation, depth estimation, and surface normal estimation exhibit high cross-task correlations. For instance, depth discontinuity is usually aligned with semantic boundaries [32], and surface normal distributions are aligned with spatial derivatives of the depth maps [21]. Thus, a number of works have been focusing on multi-task dense predictions [10, 20, 25, 32, 35, 36, 37, 38, 39, 41, 45, 46, 47]. They leverage parameters sharing to conduct cross-task interactions by effective attention mechanisms for task feature selection [20], and multi-modal distillation [35], multi-scale cross-task interactions [32], global pixel and task interactions [37] and multi-task mixture-of-experts [38]. However, these works focus on fully-supervised settings. In contrast, our work addresses the challenge of insufficient supervision signals in each task.

**Semi-supervised learning.** Obtaining pseudo labels for semi-supervised learning is a popular research direction, with several deep learning works published on the topic [13, 15, 18, 26, 28, 30, 34, 48, 49]. Among them, [15] aims at picking up the class which has the maximum predicted confidence. The graph-based label propagation method [13] is also used to infer pseudo-labels for unlabeled data. [26] provides a confidence level for each unlabeled sample to reduce influences from outliers and uncertain samples, and uses MMF regularization at feature levels to make images with the same label close to each other in the feature space. [34] uses accurate pseudo labels produced by the teacher model on clean unlabeled data to train the student model with noise injected. For dense prediction tasks, such as semantic segmentation, several works focus on assigning pixel-wise pseudo annotations from high-confidence predictions [18, 48, 49]. However, these works target single-task learning setups. Despite pseudo labeling, discovering consistency for regularization is also a popular direction for unlabeled data [17, 22, 29, 44]. [17, 22, 44] focus on building cross-task consistency, while [29] uses image-level feature similarities to find important samples for semi-supervised learning. Differently, our work targets *pixel-level* task supervision discovery by hierarchical task tokens containing multi-level multi-task representations for partially annotated dense predictions.

**Multi-task Partially Supervised Learning.** As discussed in the introduction, obtaining pixel-level annotations for every task on images is prohibitively expensive. Therefore, some recent works focus on partially annotated settings for multi-task learning [12, 17, 19, 21, 22, 33, 40, 42, 44]. Since directly recovering labels from other tasks is an ill-posed problem [17], enforcing consistency among tasks is usually adopted. For instance, constructing a common feature space to align predictions and impose regularization [17], and leveraging intrinsic connections of different task pairs between predictions of different tasks on unlabeled data in a mediator dataset, when jointly learning multiple models [21]. Adversarial training is also adopted to align the distributions between labeled and unlabeled data by discriminators [33]. To the best of our knowledge, our hierarchical task tokens for both pseudo feature supervision and task label discovery are a novel exploration of the problem, and show a clear difference from existing works.

## 3 Proposed Method

Our proposed approach for learning Hierarchical Task Tokens (HiTTs) primarily comprises two stages, *i.e.*, the Global Token Learning and the Fine-grained Token Learning. The overall structure of HiTTs is depicted in Fig. 2. Firstly, in the Global Token Learning stage, the global task tokens produce task features and then learn rich task-level representations by conducting inter- and intra-task interactions with all task features. The global tokens are utilized to exploit rich representations in feature space and discover feature-level pseudo supervision. Subsequently, in the fine-grained stage, we project each task feature into fine-grained feature space by simple convolution layers, and derive the fine-grained tokens from the global tokens by Multi-layer Perceptrons (MLPs), to inherit well-learned global task representations and therefore achieve consistent pseudo label discovery. To perform a uniform confidence-based pseudo label discovery for different types of dense prediction tasks, we follow [2] to conduct discrete quantization of regression task annotations (e.g. depth estimation and normal estimation), and treat all tasks as pixel-wise classification.

### 3.1 Global Task Token Learning

In the global task token learning stage, we target learning global tokens representing the distributions of each task, which are further used for pseudo feature supervision discovery. The learning process is mainly achieved

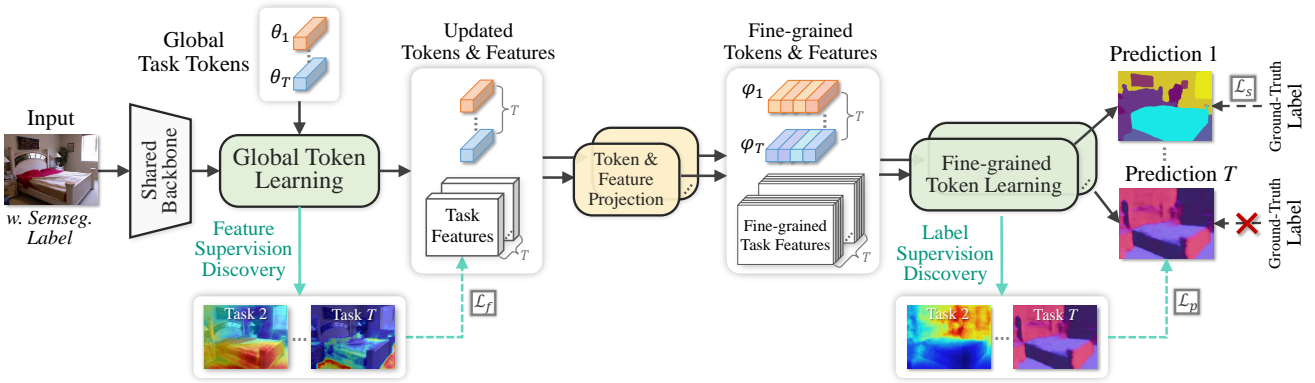


**Fig. 2** Illustration of our method. HiTTs consist of both global and fine-grained task tokens which learn discriminative task representations by conducting feature-token interactions with attentions in corresponding multi-task decoding stages. The global task tokens  $\theta_i$  discover feature-level pseudo supervision  $\mathcal{L}_f$ , while the fine-grained task tokens  $\varphi_i$  inherit the knowledge from global task tokens and directly discover pixel labels for supervision  $\mathcal{L}_p$ . The supervision from ground-truth label is denoted as  $\mathcal{L}_s$ .

by inter- and intra-task interactions among tokens and features, in order to exploit beneficial multi-task representations for token learning and feature supervision discovery.

Given an RGB input  $\mathbf{X} \in \mathbb{R}^{3 \times H \times W}$ , a multi-task dense prediction framework firstly produces a task-generic representation  $\mathbf{F}_s \in \mathbb{R}^{C \times h \times w}$  through a shared encoder. Considering we have  $T$  tasks, and we target decoding task features  $\{\mathbf{F}_1, \mathbf{F}_2, \dots, \mathbf{F}_T\}$  from  $\mathbf{F}_s$  as well as learning representative global task tokens  $\{\theta_1, \theta_2, \dots, \theta_T\}$  for each task.

As shown in Fig. 3, the proposed global task token learning process is mainly composed of three stages: i) Inter-Task Learning, which aims to learn explicit global cross-task token affinities  $\mathbf{A}$ , and conduct cross-task interaction accordingly for the global token learning process. ii) Intra-task Learning, which learns task-specific information by globally conducting self-attention between task feature and token pairs. iii) Feature Supervision Discovery: excavating pseudo feature supervision for unsupervised task features by exploiting global task tokens.

Firstly, we flatten the shared feature  $\mathbf{F}_s$  into feature tokens with shape  $\mathbb{R}^{C \times (hw)}$ , and use each global task token to query the shared feature to obtain each task feature  $\mathbf{F}_i$  accordingly. Then, to conduct *inter-task learning*, all global task tokens are used to produce cross-task affinities that explicitly guide the learning process. The cross-task affinity map  $\mathbf{A} \in \mathbb{R}^{T \times T}$  is calculated as:

$$\mathbf{A} = \text{Softmax}(\mathbf{Q} \times \mathbf{K}^\top), \quad (1)$$

where  $\mathbf{Q}$  and  $\mathbf{K}$  are individual linear projection of concatenated global tokens  $\Theta = [\theta_1; \theta_2; \dots; \theta_T]^\top$ , in which  $[\cdot]$  indicates the concatenation. After affinity matrix  $\mathbf{A}$  is calculated, it is used to conduct affine combinations

of task features and global task tokens respectively:

$$\Theta' = \mathbf{A} \times \Theta, \quad \mathcal{F}' = \mathbf{A} \times \mathcal{F}, \quad (2)$$

and similarly,  $\mathcal{F} = [\mathbf{F}_1; \mathbf{F}_2; \dots; \mathbf{F}_T]^\top$ , and  $\Theta', \mathcal{F}'$  represents all updated task tokens and features after the affine combinations. For each task feature  $\mathbf{F}_i$ , if it is not directly supervised by labels, the feature will be less representative and contain more noise. Thus, conducting affine combinations among all tasks ensures that the task-shared representations from labeled tasks are able to fertilize the unlabeled task features.

Afterward, the updated tokens and features with cross-task information are involved in the *intra-task learning*, where we first concatenate every corresponding task token and feature, and perform self-attention on the spatial dimension among each token-feature pair  $[\theta'_i; \mathbf{F}'_i] \in \mathbb{R}^{C \times (hw+1)}$ . The global task tokens will further learn more specific and discriminative task representations during this process, and representative task tokens will in turn enhance the feature quality as well. Followingly, we discover pseudo feature supervision with the aid of well-learned global task tokens  $\theta'_i$ , and this process will be discussed in Sec. 3.3.

Additionally, for multi-scale backbone features, directly fusing them ignores the various granularity of task representations maintained at different scales. Thus, for multi-scale image backbone, we further propose Multi-scale Global Task Token Learning in order to learn comprehensive multi-scale task relations. The proposed method involves *inter-task learning* separately at each scale, and then the multi-scale features and tokens are fused before *intra-task learning*. In this way, the global task tokens gain richer cross-task relations at different scales and are able to maintain stronger representations. We will illustrate this part in detail in the supplementary material.

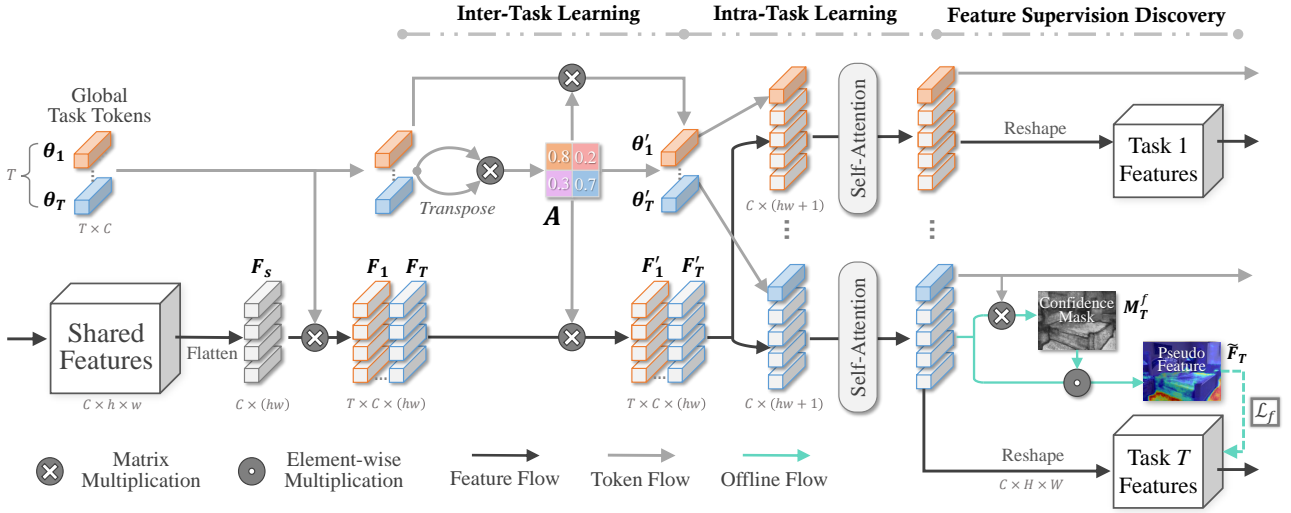


**Fig. 3** Illustration of the Global Task Token Learning, which mainly contains three stages: (i) Inter-Task Learning: predicting cross-task token affinities  $A$  from the global task tokens. (ii) Intra-Task Learning: conducting self-attention between task features and tokens. (iii) Feature Supervision Discovery: excavating pseudo feature supervision based on the learned task tokens and attentions.

### 3.2 Fine-grained Task Token Learning

After the global task tokens are learned, we further propose to conduct feature-token interaction at a finer spatial granularity, which takes advantage of various representations in global task tokens and boosts task label discovery process. The process is illustrated in Fig. 4.

Firstly, we jointly project each updated task token  $\theta'_i \in \mathbb{R}^C$  and feature  $F'_i \in \mathbb{R}^{C \times h \times w}$  into the prediction space with finer granularity. For features, this can be easily achieved by applying a linear convolution layer, and we denote the fine-grained task features as  $G_i \in \mathbb{R}^{C_p \times H \times W}$ , where  $C_p$  indicates the prediction dimension. For tokens, we denote the projected fine-grained tokens as  $\varphi_i \in \mathbb{R}^{C_p \times C}$ , we hope every  $1 \times C$  vector inside it can represent one category distribution over the spatial dimension. The simplest way is to project each  $\theta'_i$  with a Multi-Layer Perceptron (MLP), which can be described as:  $\varphi_i = \text{MLP}_i(\theta'_i)^\top, i = 1, 2, \dots, T$ . However, since there are no direct supervision imposed during this process to distinguish the learned fine-grain tokens, the MLPs will tend to degenerate and perform linearly correlated outputs, which prevents the fine-grained tokens from learning discriminative task-specific representations. To alleviate this problem, we propose to use Orthogonal Embeddings (OE) to serve as priors and aid the learning process of fine-grained tokens.

In order to learn discriminative task representations, the vectors in the fine-grained token should be far from each other to represent meaningful and distinguishable task category information, so we use a group of orthogonal basis in  $\mathbb{R}^{C_p}$  to serve as the embedding for MLP

input, denoting as  $\mathbf{o} \in \mathbb{R}^{C_p \times C_p}$ . These OE are projected into the feature space by linear projection matrix  $\mathbf{W}_i^o \in \mathbb{R}^{C \times C_p}$ , and then added with the global token before being fed into the MLP. The process can be described as:

$$\varphi_i = \text{MLP}_i(\mathbf{W}_i^o \times \mathbf{o} + \underbrace{[\theta'_i; \theta'_i; \dots; \theta'_i]}_{C_p})^\top. \quad (3)$$

With the prior information from  $\mathbf{o}$ , the MLPs are capable of keeping the distance between the vectors in  $\varphi_i$  far from each other in the feature space, which makes it able to learn information that distinguishes between task categories as well as inherit the global representations in  $\theta'_i$ .

Subsequently, we exploit the fine-grained task tokens  $\varphi_i$  for the fine-grained token learning process. Normally,  $G_i$  is noisy and low-confident on unlabeled data due to the lack of supervision, which leads to inaccurate predictions. Since we are treating all of the tasks as pixel-wise classification, we propose to use fine-grained task tokens to encourage  $G_i$  to produce high-confident logits, and enhance the quality of pseudo labels:

$$G'_i = \text{Conv}_i^{3 \times 3}(G_i \odot \text{Softplus}(\varphi_i \times G_i)), \quad (4)$$

where  $\text{Softplus}(x) = \log(1 + \exp(x))$ , and  $\text{Softplus}(\varphi_i \times G_i)$  gives pixel-wise positive score masks on each channel of  $G_i$ . Since  $\varphi_i$  inherits global task representations from  $\theta'_i$ , which will perform more robustly on unlabeled data, and aid the production of distinguished logits score in the updated feature  $G'_i$ , as well as high-confident final task predictions. Similar to the previous stage, we also conduct pseudo label discovery after the

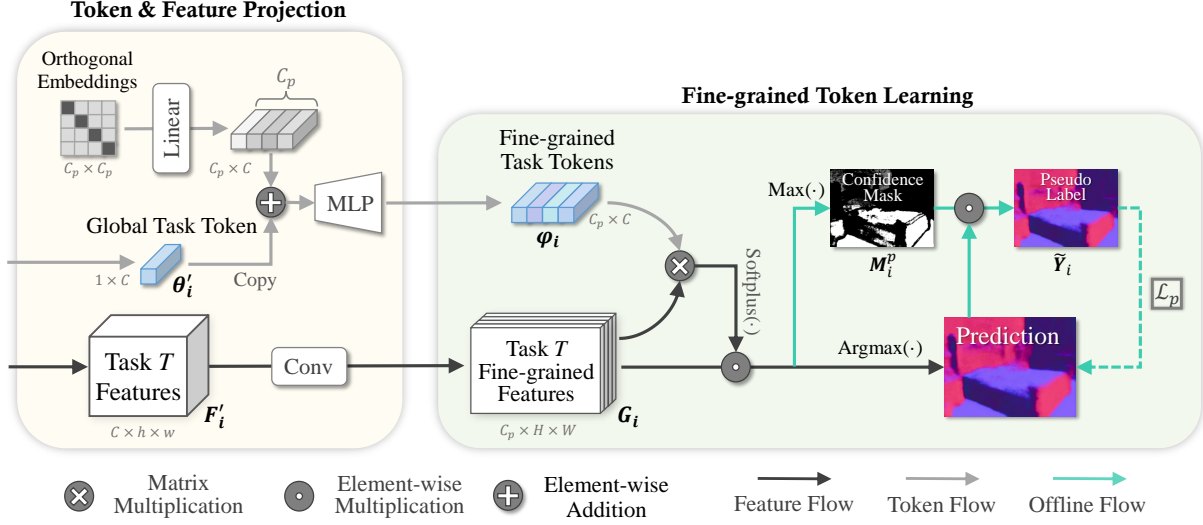


**Fig. 4** Illustration of Token & Feature Projection and the Fine-grained Task Token Learning. Different tasks have the same structure, and we take one task as example. We firstly project the fine-grained feature  $G_i$  from the updated task feature  $F'_i$ , and derive fine-grained task tokens  $\varphi_i$  from the updated global task tokens  $\theta'_i$ . Then, we produce final task predictions with pseudo label discovery by conducting interactions between  $G_i$  and  $\varphi_i$ .

fine-grained tokens are learned, which will be discussed in detail in the next section.

### 3.3 Hierarchical Label Discovery and Multi-task Optimization

For the multi-task partially annotated setting, the training loss on labeled data can be described as:

$$\mathcal{L}_s = \frac{1}{T} \sum_{i=1}^T \left( \alpha_i L_i \left( \hat{Y}_i, Y_i \right) \right), \quad (5)$$

where where  $L_i(\cdot)$  is the loss function for task  $i$ , and  $\alpha_i = 1$  if task  $i$  has ground-truth label, otherwise  $\alpha_i = 0$ .  $\hat{Y}_i$  and  $Y_i$  are task prediction and ground-truth.

We firstly train the multi-task model with HiTTs jointly with  $L_i$  only to achieve convergence on labeled data, then we utilize both hierarchies of tokens to discover feature-level and prediction-level pseudo supervision. As we mentioned in Sec. 3.1, before the updated tokens and features are fed into the next stage, we conduct the *feature supervision discovery* to excavate feature-level supervision signals for unlabeled tasks. As shown in Fig. 3, we use the updated global task tokens to query each pixel feature on every task and produce confidence mask  $M_i^f = \text{Sigmoid}(\theta_i'^{\top} \times F'_i)$ . Since  $\theta_i$  is globally learned on all task features, in  $M_i^f$ , higher scores indicate that the pixel features have a higher response to task  $i$ , which should be further used to prove task supervision. Thus we use  $M_i^f$  to serve as a soft

confidence mask for pixel-wise feature supervision loss:

$$\mathcal{L}_f = \frac{1}{T} \sum_{i=1}^T \left( \alpha_i L_{\text{mse}} \left( F'_i, \tilde{F}_i \right) + (1 - \alpha_i) M_i^f \odot L_{\text{mse}} \left( F'_i, \tilde{F}_i \right) \right), \quad (6)$$

where  $\tilde{F}_i$  represents the offline saved features which serve as pseudo supervision signals for unsupervised task features. The  $\odot$  represents element-wise multiplication,  $L_{\text{mse}}$  is the mean squared error loss for feature distance measurement. For the feature loss on labeled task (first item in Eq 6), we regard all pixel features from  $\tilde{F}_i$  as valid since they are supervised by ground-truth label, while for unlabeled task (second item in Eq 6), we use  $M_i^f$  encourage high-confidence pixel features and depress low-confidence ones.

Afterward, we also conduct *pseudo label discovery* with the aid of well-learned fine-grained task tokens  $\varphi_i$  as mentioned in Sec. 3.2. We directly produce pseudo labels from  $G'_i$ :  $\hat{Y}_i = \text{Argmax}(\text{Softmax}(G'_i))$ , along with binary masks to select high confidence pixel pseudo labels:  $M_i^p = \text{Max}(\text{Softmax}(G'_i)) > \tau_i$ , where  $\tau_i$  is a threshold used to produce binary masks. The loss for pseudo label supervision can be written as:

$$\mathcal{L}_p = \frac{1}{T} \sum_{i=1}^T \left( (1 - \alpha_i) M_i^p \odot L_i \left( \hat{Y}_i, Y_i \right) \right), \quad (7)$$

Finally, we sum all of the losses in Eq 5, 6 and 7 to supervise all task features and predictions. The overall

losses to optimize the model can be described as:

$$\begin{aligned} \mathcal{L} &= \mathcal{L}_s + \mathcal{L}_p + \mathcal{L}_f \\ &= \frac{1}{T} \sum_{i=1}^T \left[ \alpha_i \left( L_i(\hat{\mathbf{Y}}_i, \mathbf{Y}_i) + L_{\text{mse}}(\mathbf{F}'_i, \tilde{\mathbf{F}}_i) \right) \right. \\ &\quad \left. + (1 - \alpha_i) \left( \mathbf{M}_i^p \odot L_i(\hat{\mathbf{Y}}_i, \tilde{\mathbf{Y}}_i) + \mathbf{M}_i^f \odot L_{\text{mse}}(\mathbf{F}'_i, \tilde{\mathbf{F}}_i) \right) \right] \end{aligned} \quad (8)$$

where the second row represents all prediction-level supervision and the third row represents all feature-level supervision.

## 4 Experiment

### 4.1 Experimental Setup

**NYUD-v2.** NYUD-v2 [27] contains 795 and 654 RGB-D indoor scene images for training and testing respectively. We use the 13-class semantic annotations which is defined in [6], the truth depth annotations recorded by Microsoft Kinect depth camera, and surface normal annotations which are produced in [8]. Following the setting in [17, 20], we use  $288 \times 384$  image resolution to speed up training. We use Adam optimizer with a learning rate of  $1 \times 10^{-4}$ , and train all models for 400 epochs with batch size 8. We update the learning rate every 100 epoch with  $\gamma = 0.5$  as the multiplying factor.

**Cityscapes.** Cityscapes [5] contains 2975 and 500 street-view images for training and testing respectively. We used the projected 7-class semantic annotations from [20], and disparity maps to serve as depth annotations. Following the setting in [17, 20], we use  $128 \times 256$  image resolution to speed up training. The optimizer and learning rate scheduler are set as the same as NYUD-v2.

**PASCAL-Context.** PASCAL-Context [9] contains 4998 and 5105 images for training and testing respectively, which also have pixel-level annotations for semantic segmentation, human-parts segmentation and semantic edge detection. Additionally, we also consider surface normal estimation and saliency detection distilled by [23]. We use Adam optimizer with learning rate  $1 \times 10^{-4}$ , and weight decay  $1 \times 10^{-4}$ , and train for 20000 steps with batch size 6. We update the learning rate by polynomial scheduler and  $\gamma = 0.9$  for the power factor.

**Model Setting.** Following [17], we use SegNet [1] for NYUD-v2 and Cityscapes, ResNet-18 [11] for PASCAL-Context as the backbone of our single task learning (STL) baselines, and the multi-task baseline (MTL) is built from it, which consists of a shared backbone encoder and several task-specific decoding heads. For the learning of HiTTs, we follow [2, 16, 43], and perform

a discrete quantization of the label space of continuous regression tasks such as Depth. and Normal. This discrete quantization does not contribute to multi-task learning performance as analysed in [2], so we ensure a fair comparison with other works. The network with HiTTs is first jointly trained only on labeled data to obtain high-quality task representations and produce pseudo labels, and then follow the self-training procedure in [34], we optimize the model with labels or pre-produced pseudo labels on all tasks and train from scratch, and the feature-level supervision is also applied during the training period.

**Data Preparation.** We follow the setting of [17, 20] to process training data, and form two partially annotated settings [17]: **(i) one-label:** for each input image, it is only associated with one task annotation; **(ii) random-labels:** each image has at least one and at most  $N - 1$  tasks with corresponding task annotations, in the set of  $N$  tasks. Additionally, we provide two extra settings to further validate the effectiveness of our method: **(iii) full-labels:** each image has labels on every task, which is the usual multi-task learning setting; **(iv) few-shot:** one certain task has only very few labels while the other tasks are fully supervised.

**Training Pipeline.** We first train the multi-task model with HiTTs on all labeled task data. Then the weights of the network and tokens are fixed, and used to produce hierarchical supervision on both feature and prediction spaces. We produce the pseudo label in an offline manner according to [34], which is labeling on clean image without data augmentation, and training on augmented images and pseudo labels to enforce consistent predictions. In [34], this method is only applied to classification tasks while we extend the utilization to general dense prediction tasks. After the pseudo labels are produced, we use them along with the ground-truth labels to jointly train the multi-task model from scratch. Additionally, we also use the pseudo feature supervision produced by this pre-trained multi-task model for feature regularization during the optimization process. Both hierarchies of the discovered supervision signals ensure that all task predictions will obtain pixel-wise supervision for multi-task optimization to gain better generalization ability on unlabeled data.

**Evaluation Metrics.** We have briefly introduced our evaluation metrics for multiple dense prediction tasks in Sec.4.1. We provide a more detailed description as follows: (i) mIoU: mean intersection over union; (ii) pAcc: per-pixel accuracy; (iii) AbS or AbR: absolute error or absolute-relative error; (iv) rmse: root mean square error (for Normal. we calculate the mean square error of the predicted angles with the ground-truths); (v) mErr: mean of angle error; (vi) odsF: optimal dataset F-

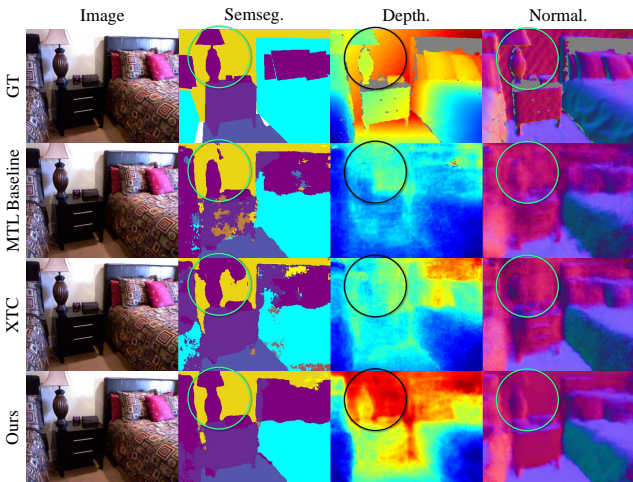


**Fig. 5** Comparisons with SoTA works on NYUDv2. Ours shows both clear semantic boundaries and accurate geometry estimations, indicating the effectiveness of cross-task feature-token interactions.

measure [24]; (vii) threshold: for surface normal estimation, we calculate the proportion of pixels with angle error smaller than three thresholds  $\eta \in \{11.25^\circ, 22.50^\circ, 30^\circ\}$ . Additionally, to better evaluate the proposed method, we also consider using  $\Delta_{MTL}$  proposed by [31] to evaluate the overall improvement of the multi-task performances of all the tasks, which is defined as:

$$\Delta_{MTL} = \sum_N (-1)^{l_t} (M_{m,t} - M_{s,t}) / M_{s,t} \quad (9)$$

where  $l_t = 1$  if a lower evaluation value indicates a better performance measurement of  $M_t$  for task  $t$ , and  $l_t = 0$  if a higher value is better. Footnote  $s$  and  $m$  represent the performance of the single-task learning and the multi-task learning respectively. We will show experimental results with all of these metrics to further show the effectiveness of our method.

## 4.2 State-of-the-art Comparison

**Comparison on NYUD-v2.** We compare our method with [17, 20] on NYUD-v2 under both the one-label and random-labels settings, and the quantitative results are shown in Table 4.1. XTC [17] is the first work designed for partially annotated multi-task dense prediction. MTAN [17] is an attention-based MTL network designed for the fully supervised setting, and we train it with our setup. The quantitative results show that our method surpasses them by a large margin on all the metrics of the three tasks. More specifically, ours achieves +9.63%  $\Delta_{MTL}$  and +8.62%  $\Delta_{MTL}$  compared with [17] under the two partial-label settings, respectively. The qualitative comparison with the state-of-

the-art method XTC [17] as shown in Fig. 5 can also confirm the superior performance of our method.

Similar to [17], our HiTTs can also be applied on full-labels setting, which utilizes cross-task relations and task-token interactions to fertilize the multi-task learning process. We compare with some of the recent works, including multi-task interaction works like MTAN [20], X-Task [42] and CCR [36]; and multi-task optimization strategies like Uncertainty [14], GradNorm [4], MGDA [7] and DWA [20]. As shown in Table 2, our method still clearly surpasses all of the SOTA works (13.29%  $\Delta_{MTL}$  overall), indicating the effective cross-task interaction brought by HiTTs. Additionally, with the aid of feature-level supervision loss  $\mathcal{L}_f$ , which is supported by global task tokens, our method can achieve 14.64%  $\Delta_{MTL}$  overall on the three tasks.

**Comparison on Cityscapes.** We also compare our results with [17, 20] on Cityscapes, under the *one-label* setting with both Semseg. and Depth. tasks. As shown in Table 3, our method achieves SOTA performance on both tasks, and significantly better performance on Depth (15.09% higher on *AbS.* compared with [17]), resulting in an average gain of +6.98% in terms of  $\Delta_{MTL}$ . Additionally, it’s worth mentioning that our work is the only one achieving balanced performance gain on both tasks compared with STL. Qualitative comparisons are shown in Fig. 6.

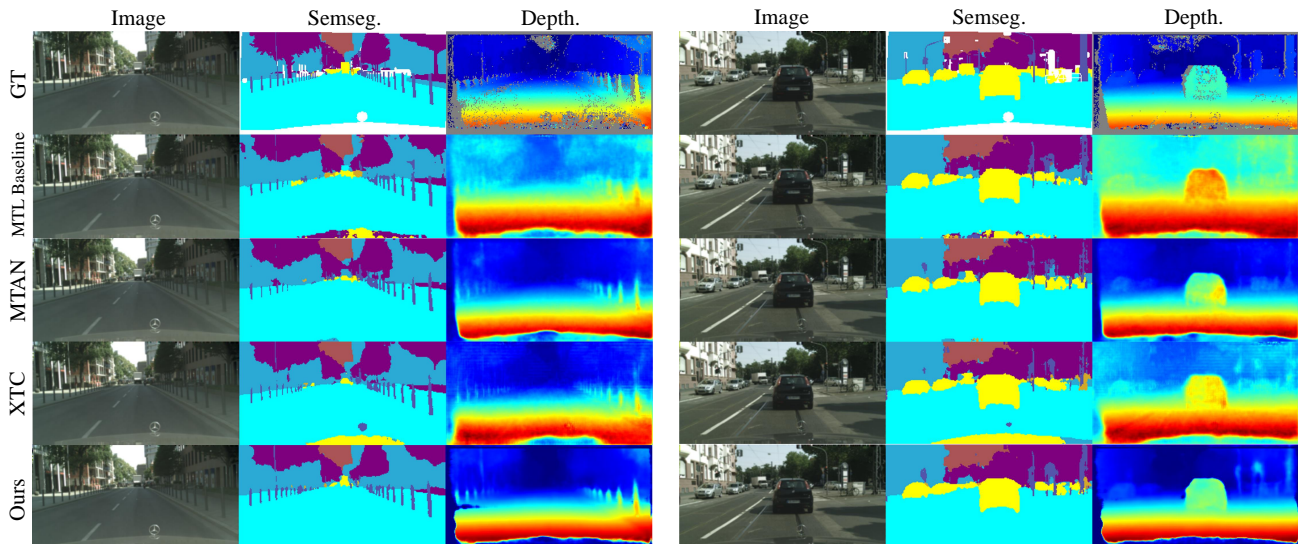
**Comparison on Pascal-Context.** For the comparison on Pascal-Context, we consider both *one-label* and *random-labels* settings. As shown in Table 4, our method achieves clear improvement over other methods on the majority of tasks under both settings. The greatest enhanced task is Semseg, which has +6.8 and +3.2 *mIoU* on the two settings compared with [17]. Overall, our method is +6.87% and +3.84% higher in terms of  $\Delta_{MTL}$  compared with [17], the gain is more significant under one-label setting with fewer labels.

## 4.3 Model Analysis

**Components of Hierarchical Task Tokens.** As shown in Table 5, under the one-label setting on NYUD-v2, we give an ablation study of our key components. Generally, we analyze the role of global task tokens  $\theta_i$  and fine-grained tokens  $\varphi_i$ , and core designs for token learning process, including the orthogonal embeddings (OE) (3.2), inter- and intra-task learning (3.1). The quantitative results clearly show that both hierarchies of tokens contribute to the multi-task performance and HiTTs boost the model performance by overall +6.40%  $\Delta_{MTL}$  on all tasks compared with baseline. Without either hierarchy of tokens, the performance drops, especially on Semseg. For the learning process of HiTTs, the orthogo-

**Table 1** Comparison on NYUD-v2 under *one-label* and *random-labels* settings. Our method shows clear performance gain over three tasks, which is consistent with the visualization results.

Setting	Model	Semseg.		Depth.		Normal.			$\Delta_{MTL}$ (%) $\uparrow$		
		$mIoU\uparrow$	$pAcc\uparrow$	$AbS\downarrow$	$rmse\downarrow$	$mErr\downarrow$	$rmse\downarrow$	$\eta_1\uparrow$		$\eta_2\uparrow$	$\eta_3\uparrow$
One-Label	STL	29.28	55.41	0.7182	1.0151	30.1971	37.7115	23.1532	46.4046	58.5216	-
	MTL <i>baseline</i>	30.92	58.23	0.5982	0.8544	31.8509	38.6313	19.7083	41.2614	53.6381	0.11
	MTAN [20]	30.92	57.14	0.6196	0.8477	30.0278	36.7808	21.4199	44.7805	57.5720	3.26
	XTC [17]	33.46	60.95	0.5728	0.8056	31.1492	37.8211	19.8410	42.2268	54.9997	3.60
	Ours	<b>35.81</b>	<b>63.22</b>	<b>0.5540</b>	<b>0.7939</b>	<b>28.5131</b>	<b>36.1738</b>	<b>26.4985</b>	<b>50.2357</b>	<b>61.8343</b>	<b>13.23</b>
Random-Labels	STL	34.49	60.52	0.6272	0.8824	27.9681	34.9293	24.6011	49.7888	62.4425	-
	MTL <i>baseline</i>	35.49	61.81	0.5503	0.7874	29.9541	36.7726	21.6933	45.0412	57.7516	-1.47
	MTAN [20]	35.96	61.64	0.6120	0.8272	28.6933	35.3528	23.0253	47.2287	60.1113	-0.48
	XTC [17]	38.11	64.37	0.5387	0.7755	29.6549	36.3992	21.7058	45.4801	58.4236	0.66
	Ours	<b>41.78</b>	<b>66.50</b>	<b>0.5177</b>	<b>0.7472</b>	<b>27.3488</b>	<b>34.6820</b>	<b>27.1619</b>	<b>51.8924</b>	<b>63.7670</b>	<b>9.28</b>

**Fig. 6** Comparisons with SOTA methods on Cityscapes.

nal embeddings (OE) are essential for generating representative fine-grained task tokens, and without OE, the performance will significantly drop ( $-4.38\% \Delta_{MTL}$ ), also especially on Semseg. which requires more discriminative category information. For the inter- and intra-task learning, both contribute to the learning process, and inter-task learning contributes more since it exploits useful representations from other tasks by cross-task feature-token interactions.

### Effect of Hierarchical Feature Supervision and Label Discovery.

We analyze the contributions from two types of pseudo supervision losses ( $\mathcal{L}_p$  for pseudo label loss and  $\mathcal{L}_f$  for feature supervision loss) on different hierarchies. As shown in Table 5, both methods boost multi-task performance:  $+9.64\% \Delta_{MTL}$  for  $\mathcal{L}_f$  and  $+11.46\% \Delta_{MTL}$  for  $\mathcal{L}_p$  compared with MTL baseline.  $\mathcal{L}_p$  contributes more since fine-grained task tokens contain more specific and discriminative task informa-

tion and are directly involved in the formation process of task predictions. The combination of both methods achieves better performance ( $+13.12\% \Delta_{MTL}$ ) than applying them separately, which validates the importance of consistently discovering supervision signals in both hierarchies. Compared with the naive pseudo-label supervision without the utilization of task tokens (denoted as  $\mathcal{L}_p^*$ ), our HiTTs-based pseudo-label discovery is much better. Since MTL *baseline* shares an image backbone that learns stronger representations on all tasks, the MTL produces pseudo labels with better quality and surpasses STL a lot in performance ( $+3.86\% \Delta_{MTL}$ ). Our HiTTs-based supervision performs i) consistent label discovery in both feature and prediction space; ii) effective cross-task feature-token interactions, which furthermore enhance the quality of pseudo labels, and bring extra  $+4.68\% \Delta_{MTL}$  overall.

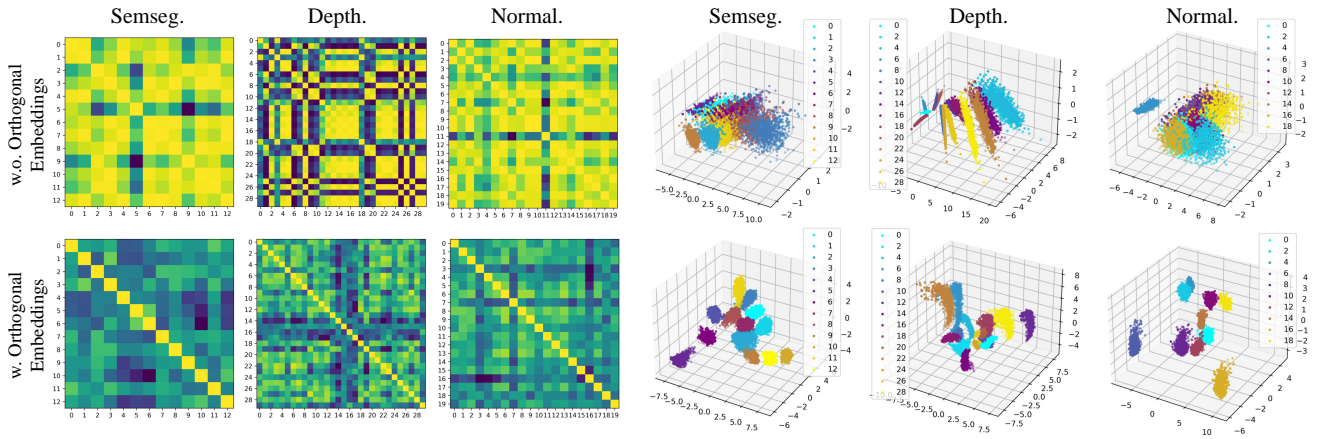


**Fig. 7** Visualization of self-affinities heatmap (*left*) and PCA for distributions (*right*) of the fine-grained task tokens of the three tasks, with samples from NYUD-v2 testing set. Based on orthogonal embeddings, the affinities between different tokens are low and the distances between different token clustering centers are far, which indicates that more discriminative representations are learned with our method.

**Table 2** Comparison on NYUD-v2 under *full-labels* settings. Our method achieves significantly better performance compared with SoTA multi-task learning works on all of the three tasks.

Model	Semseg. $mIoU\uparrow$	Depth. $AbS\downarrow$	Normal. $mErr\downarrow$	$\Delta_{MTL}$ (%) $\uparrow$
STL	37.45	0.6079	25.94	-
MTL <i>baseline</i>	36.95	0.5510	29.51	-1.91
MTAN [20]	39.39	0.5696	28.89	0.03
X-Task [42]	38.91	0.5342	29.94	0.20
Uncertainty [14]	36.46	0.5376	27.58	0.87
GradNorm [4]	37.19	0.5775	28.51	-1.87
MGDA [7]	38.65	0.5572	28.89	0.06
DWA [20]	36.46	0.5429	29.45	-1.83
XTC [17]	41.00	0.5148	28.58	4.87
XTC+ [14]	41.09	0.5090	26.78	7.58
CCR [36]	43.09	0.4894	27.87	9.04
Ours	44.32	0.4813	25.76	13.29
Ours+ $\mathcal{L}_f$	<b>45.47</b>	<b>0.4763</b>	<b>25.72</b>	<b>14.64</b>

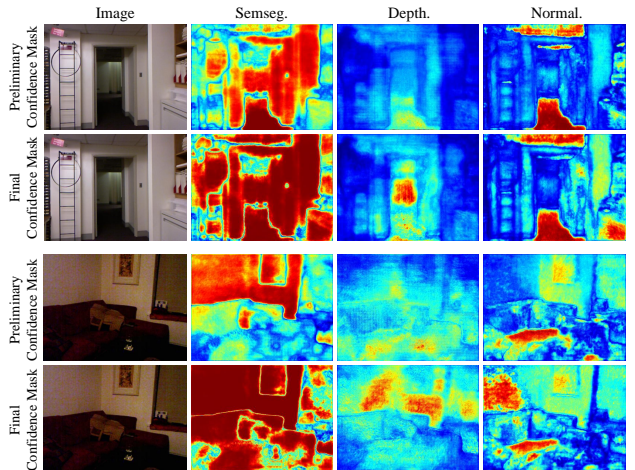


**Fig. 8** Comparison of the task confidence map before and after refined by the fine-grained task tokens, which greatly encourage high-confidence predictions on all tasks (red color represents high-confidence areas). For noisy data like the second photo taken in a dark environment, this enhancement are more significant.

**Table 3** Comparison on Cityscapes under *one-label* setting.

Setting	Model	Semseg.		Depth.		$\Delta_{MTL}$ (%) $\uparrow$
		$mIoU\uparrow$	$pAcc\uparrow$	$AbS\downarrow$	$rmse\downarrow$	
One-Label	STL	69.69	91.91	0.0142	0.0271	-
	MTL <i>baseline</i>	69.94	91.62	0.0159	0.0292	-4.92
	MTAN [20]	71.12	92.35	0.0146	0.0278	-0.72
	XTC [17]	73.23	92.73	0.0159	0.0293	-3.53
	Ours	<b>73.65</b>	<b>92.81</b>	<b>0.0135</b>	<b>0.0265</b>	<b>3.45</b>

**Learning Effect on Unlabeled Data.** We also study the performance of our method on the labeled and unlabeled data separately on NYUD-v2 training set under one-label setting. As shown in Table 6, for data without labels, model with HiTTs generalizes better on them,

especially on Depth. and Normal, and imposing hierarchical supervision can significantly boost the performance on unlabeled data.

**Effect of Cross-Task Interactions.** To further show the effect of cross-task learning brought by HiTTs, we develop new **few-shot** settings, under which one task has only a few labels while other tasks are fully labeled. We apply this setting respectively on the three tasks of NYUD-v2, namely **few-shot-semseg**, **few-shot-depth** and **few-shot-normal**. For each few-shot task, we have 10 shots for the model to learn. As shown in Table 7, we only show the performance of the few-shot tasks in the table, and due to the lack of label supervision, the STL performs poorly on each few-shot

**Table 4** Quantitative comparison on PASCAL-Context under the *one-label* and *random-labels* setting. The *ssl* represents the semi-supervised learning strategy adopted in [17], the *CL* and *DL* are the Contrastive Loss and Discriminator Loss in [17].

Setting	Model	Semseg. <i>mIoU</i> ↑	Parsing. <i>mIoU</i> ↑	Norm. <i>mErr</i> ↓	Sal. <i>mIoU</i> ↑	Edge. <i>odsF</i> ↑	$\Delta_{MTL}$ (%)↑
One-Label	STL	47.7	56.2	16.0	61.9	64.0	-
	MTL <i>baseline</i>	48.4	55.1	16.0	61.6	66.5	0.59
	MTL <i>ssl</i> [17]	45.0	54.0	16.9	61.7	62.4	-3.60
	MTL <i>w. CL</i> [17]	48.5	55.4	17.1	61.3	64.6	-1.33
	MTL <i>w. DL</i> [17]	48.2	56.0	17.1	61.7	64.7	-1.08
	XTC [17]	49.5	55.8	17.0	61.7	65.1	-0.36
	Ours	<b>56.3</b>	<b>57.3</b>	<b>15.4</b>	<b>63.0</b>	<b>68.5</b>	<b>6.51</b>
Random-Labels	STL	60.9	55.3	14.7	64.8	66.8	-
	MTL <i>baseline</i>	58.4	55.3	16.0	63.9	67.8	-2.57
	MTL <i>ssl</i> [17]	59.0	<b>55.8</b>	15.9	64.0	66.9	-2.29
	MTL <i>w. CL</i> [17]	59.0	55.3	16.0	63.8	67.8	-2.40
	MTL <i>w. DL</i> [17]	57.9	55.2	16.2	63.4	67.4	-3.31
	XTC [17]	59.0	55.6	15.9	64.0	67.8	-2.10
	Ours	<b>62.2</b>	55.7	<b>14.7</b>	<b>64.8</b>	<b>70.7</b>	<b>1.74</b>

**Table 5** Investigate the effectiveness of different components on NYUD-v2 testing set under *one-label* setting. Inter- and Intra-Task Learning are two key components in the Global Task Token Learning stage, and Orthogonal Embeddings are the key components in the Fine-grained Task Token Learning stage.  $\mathcal{L}_f$  and  $\mathcal{L}_p$  are HiTTs-based supervision signals imposing on feature spaces and predictions respectively, and  $\mathcal{L}_p^*$  is naive pseudo label supervision without task tokens.

Method	Semseg.		Depth.		Normal.			$\Delta_{MTL}$ (%)↑		
	<i>mIoU</i> ↑	<i>pAcc</i> ↑	<i>AbS</i> ↓	<i>rmse</i> ↓	<i>mErr</i> ↓	<i>rmse</i> ↓	$\eta_1$ ↑		$\eta_2$ ↑	$\eta_3$ ↑
STL	29.28	55.41	0.7182	1.0151	30.1971	37.7115	23.1532	46.4046	58.5216	-
MTL <i>baseline</i>	30.92	58.23	0.5982	0.8544	31.8509	38.6313	19.7083	41.2614	53.6381	0.11
HiTTs	32.48	59.61	0.5844	0.8382	30.0847	37.5827	23.9975	46.4790	58.2146	6.51
<i>w/o.</i> Orthogonal Embeddings	27.38	55.08	0.6049	0.8626	30.5904	38.1046	23.5233	45.7012	57.1902	2.13
<i>w/o.</i> Inter-Task Learning	31.26	57.99	0.5966	0.8592	30.2911	37.7714	22.7802	46.2590	58.0880	4.51
<i>w/o.</i> Intra-Task Learning	31.44	58.50	0.5910	0.8533	30.1432	37.6719	23.3251	46.4354	58.1508	5.23
<i>w/o.</i> Global Task Tokens $\theta_i$	30.03	58.21	0.5823	0.8389	30.0005	37.3750	23.4160	46.1824	58.2909	5.08
<i>w/o.</i> Fine-grained Task Tokens $\varphi_i$	30.53	57.18	0.5842	0.8565	30.0891	37.4465	23.2297	45.9603	58.0509	4.60
STL <i>w.</i> $\mathcal{L}_p^*$	30.78	58.94	0.6693	0.9362	30.2420	37.8601	23.5830	46.4743	58.3739	3.03
MTL <i>w.</i> $\mathcal{L}_p^*$	33.59	61.79	0.5882	0.8554	29.8174	36.9781	23.2875	45.8803	58.1061	6.89
HiTTs <i>w.</i> $\mathcal{L}_f$	33.24	60.74	0.5708	0.8200	29.2227	36.9305	25.7968	48.8173	60.2608	9.75
HiTTs <i>w.</i> $\mathcal{L}_p$	35.22	62.93	0.5613	0.8014	28.8852	36.4316	25.3873	49.1251	60.9806	11.57
HiTTs <i>w.</i> $\mathcal{L}_p + \mathcal{L}_f$	<b>35.81</b>	<b>63.22</b>	<b>0.5540</b>	<b>0.7939</b>	<b>28.5131</b>	<b>36.1738</b>	<b>26.4985</b>	<b>50.2357</b>	<b>61.8343</b>	<b>13.23</b>

task: 5.80 *mIoU* on Semseg, 0.9633 *AbS* on Depth, and 47.5281 *mErr* on Normal. Benefiting from the sharing backbone, MTL *baseline* performs much better, since the backbone can be fully supervised on the other two tasks, and gain stronger representations from other tasks. With the aid of HiTTs, the multi-task model can achieve an extra performance gain, since the cross-task interactions brought by intra-task learning can fertilize the unlabeled tasks in the decoding stage, which introduces more task-relevant information and discriminative representations to task features without label supervision. The gains brought by HiTTs are +7.76% on Semseg, +14.86% on Depth, and +0.49% on Normal respec-

tively. Additionally, if we add the pseudo supervision signals to aid the learning process, the performance will be further improved: +19.82% on Semseg, +19.63% on Depth, and +3.85% on Normal compared with MTL *baseline*.

**Visualization Results.** We visualize: i) The distributions of fine-grained task tokens on each task in Fig. 7, with the aid of OE, the self-correlation map of tokens will be more diagonal, and the distributions after PCA have better clusters in 3-dimensional feature space. ii) The contribution of fine-grained tokens  $\varphi_i$  to the confidence map, we visualize the confidence map  $\mathcal{M}_i^p$  in Fig. 8, compared with the preliminary confidence masks

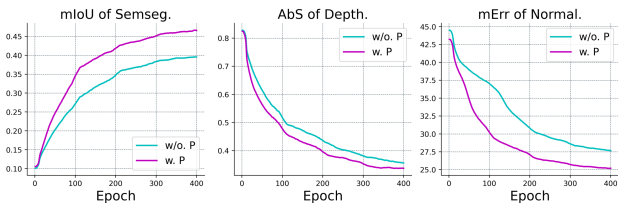
**Table 6** Investigate the performance on labeled and unlabeled data on NYUD-v2 training set under the *one-label* setting. *GT* and *pseudo* represents the ground-truth and the pseudo supervision, respectively. Our method clearly shows effective learning on unlabeled training data.

Method	Supervision		Semseg.		Depth.		Normal.				
	<i>GT</i>	<i>Pseudo</i>	<i>mIoU</i> ↑	<i>pAcc</i> ↑	<i>AbS</i> ↓	<i>rmse</i> ↓	<i>mErr</i> ↓	<i>rmse</i> ↓	$\eta_1$ ↑	$\eta_2$ ↑	$\eta_3$ ↑
MTL <i>baseline</i>	✓	✗	89.00	96.04	0.2041	0.3434	25.9280	32.0824	25.8276	52.0758	65.4135
	✗	✗	34.31	61.56	0.5823	0.8375	31.7697	38.5071	19.5042	41.2401	53.8490
HiTTs	✓	✗	86.04	95.00	0.3016	0.4625	21.7911	28.9368	38.8125	63.6280	73.8326
	✗	✗	34.69	61.48	0.5699	0.8319	29.8920	37.3331	23.9788	46.4809	58.4659
HiTTs w. $\mathcal{L}_p + \mathcal{L}_f$	✓	✗	86.63	94.89	0.3173	0.4770	20.9220	28.1260	41.2846	66.0712	75.6904
	✗	✓	<b>37.25</b>	<b>63.72</b>	<b>0.5563</b>	<b>0.8074</b>	<b>28.5169</b>	<b>36.1536</b>	<b>26.4528</b>	<b>50.0344</b>	<b>61.5778</b>

**Table 7** Investigate the cross-task learning effect on NYUD-v2 under the *few-shot* setting.

Method	Few-Shot-Semseg.		Few-Shot-Depth.		Few-Shot-Normal.				
	<i>mIoU</i> ↑	<i>pAcc</i> ↑	<i>AbS</i> ↓	<i>rmse</i> ↓	<i>mErr</i> ↓	<i>rmse</i> ↓	$\eta_1$ ↑	$\eta_2$ ↑	$\eta_3$ ↑
STL	5.80	26.06	0.9533	1.2907	47.5281	53.6422	5.4343	17.8888	27.9915
MTL <i>baseline</i>	16.75	41.01	0.9165	1.2968	40.0456	<b>46.3370</b>	12.0348	26.8520	37.2863
HiTTs	18.05	44.69	0.7803	1.1272	39.8508	47.1113	14.1108	29.4719	39.5924
HiTTs w. $\mathcal{L}_p + \mathcal{L}_f$	<b>20.07</b>	<b>45.62</b>	<b>0.7366</b>	<b>1.0206</b>	<b>38.5029</b>	46.9907	<b>17.1082</b>	<b>34.7171</b>	<b>45.1765</b>

Training Phase (*Random-Labels*):



Testing Phase (*Random-Labels*):

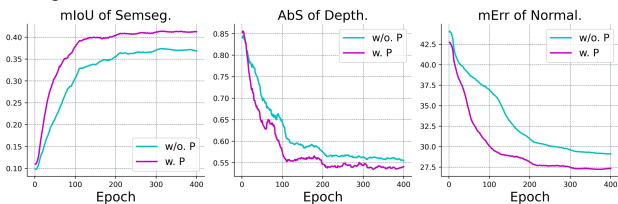


**Fig. 9** Comparison of the training and testing performance on each task with and without hierarchical Pseudo Supervision (P). The model trained with pseudo supervision converges faster on both train and test splits, and gains better performance.

without fine-grained tokens  $\varphi_i$ , the final masks have higher confidence scores after the refinement. iii) The learning curves of metrics on every task in Fig. 9, both training and testing performance are boosted consistently on all tasks with the discovered pseudo supervision (P) on both hierarchies. iv) The visual quality of pseudo labels generated by fine-grained tokens  $\varphi_i$  on Cityscapes are shown in Fig. 10. v) The visualization

**Table 8** Comparison of computational cost on NYUD-v2. All of the methods use the same SegNet [1] backbone.

Model	Params (M)	FLOPs (G)	Memory (G)
MTL <i>baseline</i>	25.06	68.81	9.36
MTAN [20]	44.23	217.26	43.46
XTC [17]	39.84	223.16	31.42
Ours	<b>25.32</b>	<b>83.14</b>	<b>21.19</b>

of score maps produced by global task tokens and fine-grained task tokens respectively on each task. As shown in Fig. 11, we conduct visualization on both NYUD-v2 and Cityscapes datasets. The score maps indicate the response of task features to task tokens, and the response patterns of feature maps on different tasks are very different, e.g. Semseg. features highlight areas with distinguish semantics, Depth. features focus on areas with a certain depth range and Normal. features focus on surfaces with the same orientation. Comparing the score maps produced by tokens from different hierarchies, we find that score maps produced by global task tokens are relatively rough and noisy, while those generated by fine-grained task tokens have finer granularity and less noise, which shows the hierarchy of the HiTTs learning process. Also, we observed that the high-lighted areas of global task tokens are monotonous, while fine-grained task tokens can high-

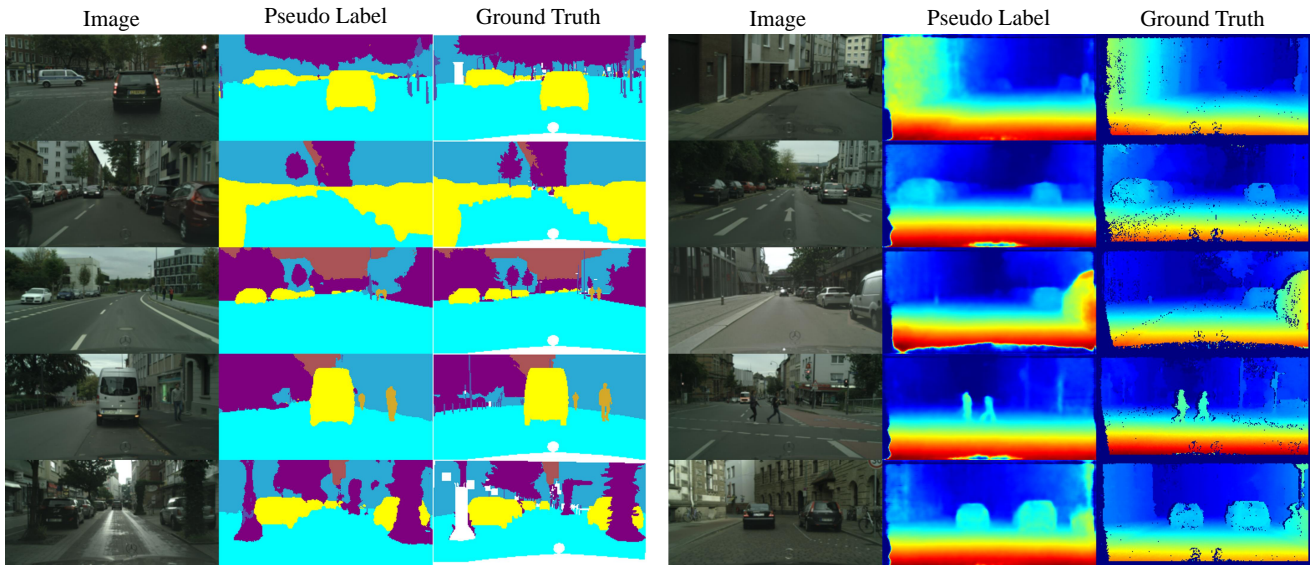


Fig. 10 Quantitative analysis of the quality of pseudo labels generated by the fine-grained task tokens on Cityscapes.

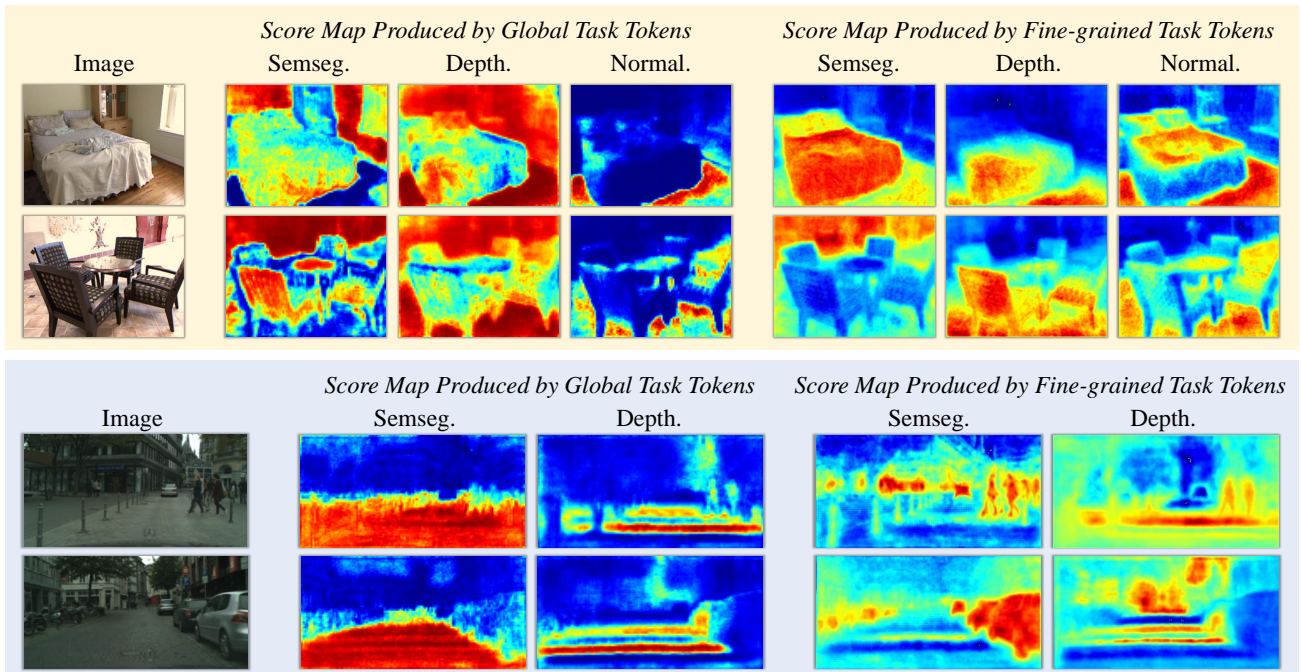


Fig. 11 Comparisons of task score maps produced by global task tokens and fine-grained task tokens. The upper part is the visualization of samples on NYUD-v2 while the lower part is on Cityscapes. The score maps indicate the response of task features to task tokens, those produced by global task tokens are relatively noisy and monotonous, while those generated by fine-grained task tokens have finer granularity and less noise, which shows the hierarchy of the HiTTs learning process.

light more various details. This phenomenon is clearly observed in Cityscapes, since the ground truths of this dataset follow the long-tail distribution, thus the global task-tokens tend to learn the category with more pixel samples, and consequently always highlight the road area as shown in Fig. 11. Oppositely, the fine-grained tokens can give attention to more details, including the vehicles and pedestrians with fewer pixel samples.

Thus, it is necessary to design a hierarchical structure for tokens to learn representations with different granularity.

**Analysis on Computational Cost.** To prove that our HiTTs are highly effective but efficient as well, in Table 8, we analyze the number of trainable parameters, average computational costs for each input image, and the total GPU memory usage during the training phase.

MTAN [20] has a complex encoding-decoding cross-task interactive structure based on attention, which causes larger model parameters and computational overhead in both the training and inference stages. [17] proposes a cross-task consistency module to regularize the training process, which causes extra parameters (+14.78M) and FLOPs (+154.35G). Our method is much less expensive compared with [17], which only requires +0.26M more parameters and +14.33G FLOPs. The total memory cost of the baseline is 9.36G. The best-performing method XTC [17] increases the memory upon the baseline to 31.42G, while ours upon the same baseline is only 21.19G, confirming the efficiency of our model.

## 5 Conclusion

In this work, we propose to learn Hierarchical Task Tokens (HiTTs) for both pseudo feature supervision and label discovery under Multi-Task Partially Supervised Learning. The global task tokens are exploited for feature-token cross-task interactions and provide feature-level supervision, while the fine-grained tokens inherit knowledge from global tokens and excavate pixel pseudo labels. Extensive experimental results on partially annotated multi-task dense prediction benchmarks validate the effectiveness of our method.

## References

1. Badrinarayanan, V., Kendall, A., Cipolla, R.: Segnet: A deep convolutional encoder-decoder architecture for image segmentation. *PAMI* **39**(12), 2481–2495 (2017) [7](#), [12](#), [16](#), [17](#)
2. Brüggemann, D., Kanakis, M., Obukhov, A., Georgoulis, S., Van Gool, L.: Exploring relational context for multi-task dense prediction. In: *ICCV*, pp. 15869–15878 (2021) [3](#), [7](#), [16](#)
3. Chen, L.C., Zhu, Y., Papandreou, G., Schroff, F., Adam, H.: Encoder-decoder with atrous separable convolution for semantic image segmentation. In: *Proceedings of the European conference on computer vision (ECCV)*, pp. 801–818 (2018) [17](#)
4. Chen, Z., Badrinarayanan, V., Lee, C.Y., Rabinovich, A.: Gradnorm: Gradient normalization for adaptive loss balancing in deep multitask networks. In: *International conference on machine learning*, pp. 794–803. *PMLR* (2018) [8](#), [10](#)
5. Cordts, M., Omran, M., Ramos, S., Rehfeld, T., Enzweiler, M., Benenson, R., Franke, U., Roth, S., Schiele, B.: The cityscapes dataset for semantic urban scene understanding. In: *CVPR*, pp. 3213–3223 (2016) [7](#)
6. Couprie, C., Farabet, C., Najman, L., LeCun, Y.: Indoor semantic segmentation using depth information. *arXiv preprint arXiv:1301.3572* (2013) [7](#)
7. Désidéri, J.A.: Multiple-gradient descent algorithm (mgda) for multiobjective optimization. *Comptes Rendus Mathématique* **350**(5-6), 313–318 (2012) [8](#), [10](#)
8. Eigen, D., Fergus, R.: Predicting depth, surface normals and semantic labels with a common multi-scale convolutional architecture. In: *ICCV*, pp. 2650–2658 (2015) [7](#)
9. Everingham, M., Van Gool, L., Williams, C.K., Winn, J., Zisserman, A.: The pascal visual object classes (voc) challenge. *IJCV* **88**, 303–308 (2009) [7](#)
10. Gao, Y., Ma, J., Zhao, M., Liu, W., Yuille, A.L.: Nddr-cnn: Layerwise feature fusing in multi-task cnns by neural discriminative dimensionality reduction. In: *CVPR*, pp. 3205–3214 (2019) [3](#)
11. He, K., Zhang, X., Ren, S., Sun, J.: Deep residual learning for image recognition. In: *CVPR*, pp. 770–778 (2016) [7](#), [16](#)
12. Imran, A.A.Z., Huang, C., Tang, H., Fan, W., Xiao, Y., Hao, D., Qian, Z., Terzopoulos, D.: Partly supervised multitask learning. *arXiv preprint arXiv:2005.02523* (2020) [3](#)
13. Iscen, A., Tolia, G., Avrithis, Y., Chum, O.: Label propagation for deep semi-supervised learning. In: *CVPR*, pp. 5070–5079 (2019) [3](#)
14. Kendall, A., Gal, Y., Cipolla, R.: Multi-task learning using uncertainty to weigh losses for scene geometry and semantics. In: *Proceedings of the IEEE conference on computer vision and pattern recognition*, pp. 7482–7491 (2018) [8](#), [10](#)
15. Lee, D.H., et al.: Pseudo-label: The simple and efficient semi-supervised learning method for deep neural networks. In: *ICML*, vol. 3, p. 896 (2013) [3](#)
16. Li, B., Dai, Y., He, M.: Monocular depth estimation with hierarchical fusion of dilated cnns and soft-weighted-sum inference. *Pattern Recognition* **83**, 328–339 (2018) [7](#), [16](#)
17. Li, W.H., Liu, X., Bilen, H.: Learning multiple dense prediction tasks from partially annotated data. In: *CVPR*, pp. 18879–18889 (2022) [1](#), [2](#), [3](#), [7](#), [8](#), [9](#), [10](#), [11](#), [12](#), [14](#), [20](#)
18. Li, Y., Yuan, L., Vasconcelos, N.: Bidirectional learning for domain adaptation of semantic segmentation. In: *CVPR*, pp. 6936–6945 (2019) [3](#)
19. Liu, Q., Liao, X., Carin, L.: Semi-supervised multitask learning. *NIPS* **20** (2007) [3](#)
20. Liu, S., Johns, E., Davison, A.J.: End-to-end multi-task learning with attention. In: *CVPR*, pp. 1871–1880 (2019) [3](#), [7](#), [8](#), [9](#), [10](#), [12](#), [14](#), [20](#)
21. Lu, Y., Pirk, S., Dlabal, J., Brohan, A., Pasad, A., Chen, Z., Casser, V., Angelova, A., Gordon, A.: Taskology: Utilizing task relations at scale. In: *CVPR*, pp. 8700–8709 (2021) [3](#)
22. Luo, X., Chen, J., Song, T., Wang, G.: Semi-supervised medical image segmentation through dual-task consistency. In: *AAAI*, vol. 35, pp. 8801–8809 (2021) [1](#), [3](#)
23. Maninis, K.K., Radosavovic, I., Kokkinos, I.: Attentive single-tasking of multiple tasks. In: *Proceedings of the IEEE/CVF conference on computer vision and pattern recognition*, pp. 1851–1860 (2019) [7](#)
24. Martin, D.R., Fowlkes, C.C., Malik, J.: Learning to detect natural image boundaries using local brightness, color, and texture cues. *PAMI* **26**(5), 530–549 (2004) [8](#)
25. Misra, I., Shrivastava, A., Gupta, A., Hebert, M.: Cross-stitch networks for multi-task learning. In: *CVPR*, pp. 3994–4003 (2016) [1](#), [3](#)
26. Shi, W., Gong, Y., Ding, C., Tao, Z.M., Zheng, N.: Transductive semi-supervised deep learning using min-max features. In: *ECCV*, pp. 299–315 (2018) [3](#)
27. Silberman, N., Hoiem, D., Kohli, P., Fergus, R.: Indoor segmentation and support inference from rgb-d images. In: *ECCV*, pp. 746–760. Springer (2012) [7](#)

28. Sohn, K., Berthelot, D., Carlini, N., Zhang, Z., Zhang, H., Raffel, C.A., Cubuk, E.D., Kurakin, A., Li, C.L.: Fix-match: Simplifying semi-supervised learning with consistency and confidence. *NIPS* **33**, 596–608 (2020) [3](#)
29. Tang, H., Jia, K.: Towards discovering the effectiveness of moderately confident samples for semi-supervised learning. In: *CVPR*, pp. 14658–14667 (2022) [3](#)
30. Tarvainen, A., Valpola, H.: Mean teachers are better role models: Weight-averaged consistency targets improve semi-supervised deep learning results. *NIPS* **30** (2017) [3](#)
31. Vandenhende, S., Georgoulis, S., Van Gansbeke, W., Proesmans, M., Dai, D., Van Gool, L.: Multi-task learning for dense prediction tasks: A survey. *PAMI* (2021) [8](#)
32. Vandenhende, S., Georgoulis, S., Van Gool, L.: Mti-net: Multi-scale task interaction networks for multi-task learning. In: *ECCV*, pp. 527–543. Springer (2020) [1](#), [3](#)
33. Wang, Y., Tsai, Y.H., Hung, W.C., Ding, W., Liu, S., Yang, M.H.: Semi-supervised multi-task learning for semantics and depth. In: *WACV*, pp. 2505–2514 (2022) [1](#), [3](#)
34. Xie, Q., Luong, M.T., Hovy, E., Le, Q.V.: Self-training with noisy student improves imagenet classification. In: *Proceedings of the IEEE/CVF conference on computer vision and pattern recognition*, pp. 10687–10698 (2020) [3](#), [7](#)
35. Xu, D., Ouyang, W., Wang, X., Sebe, N.: Pad-net: Multi-tasks guided prediction-and-distillation network for simultaneous depth estimation and scene parsing. In: *CVPR*, pp. 675–684 (2018) [1](#), [3](#)
36. Yang, S., Ye, H., Xu, D.: Contrastive multi-task dense prediction. In: *Proceedings of the AAAI Conference on Artificial Intelligence (AAAI)* (2023) [3](#), [8](#), [10](#)
37. Ye, H., Xu, D.: Inverted pyramid multi-task transformer for dense scene understanding. *ECCV* (2022) [1](#), [3](#)
38. Ye, H., Xu, D.: Taskexpert: Dynamically assembling multi-task representations with memorial mixture-of-experts. In: *Proceedings of the IEEE/CVF International Conference on Computer Vision*, pp. 21828–21837 (2023) [3](#)
39. Ye, H., Xu, D.: Taskprompter: Spatial-channel multi-task prompting for dense scene understanding. In: *ICLR* (2023) [3](#)
40. Ye, H., Xu, D.: Diffusionmtl: Learning multi-task denoising diffusion model from partially annotated data. In: *CVPR* (2024) [3](#)
41. Ye, H., Xu, D.: Invpt++: Inverted pyramid multi-task transformer for visual scene understanding. *IEEE Transactions on Pattern Analysis and Machine Intelligence (TPAMI)* (2024) [3](#)
42. Zamir, A.R., Sax, A., Cheerla, N., Suri, R., Cao, Z., Malik, J., Guibas, L.J.: Robust learning through cross-task consistency. In: *CVPR*, pp. 11197–11206 (2020) [1](#), [3](#), [8](#), [10](#)
43. Zeisl, B., Pollefeys, M., et al.: Discriminatively trained dense surface normal estimation. In: *ECCV*, pp. 468–484. Springer (2014) [7](#), [16](#)
44. Zeng, Y., Zhuge, Y., Lu, H., Zhang, L.: Joint learning of saliency detection and weakly supervised semantic segmentation. In: *ICCV*, pp. 7223–7233 (2019) [1](#), [3](#)
45. Zhang, J., Fan, J., Ye, P., Zhang, B., Ye, H., Li, B., Cai, Y., Chen, T.: Bridgenet: Comprehensive and effective feature interactions via bridge feature for multi-task dense predictions. *arXiv preprint arXiv:2312.13514v2* (2024) [3](#)
46. Zhang, Z., Cui, Z., Xu, C., Jie, Z., Li, X., Yang, J.: Joint task-recursive learning for semantic segmentation and depth estimation. In: *ECCV*, pp. 235–251 (2018) [1](#), [3](#)
47. Zhang, Z., Cui, Z., Xu, C., Yan, Y., Sebe, N., Yang, J.: Pattern-affinitive propagation across depth, surface normal and semantic segmentation. In: *CVPR*, pp. 4106–4115 (2019) [3](#)
48. Zou, Y., Yu, Z., Kumar, B., Wang, J.: Unsupervised domain adaptation for semantic segmentation via class-balanced self-training. In: *ECCV*, pp. 289–305 (2018) [3](#)
49. Zou, Y., Yu, Z., Liu, X., Kumar, B., Wang, J.: Confidence regularized self-training. In: *ICCV*, pp. 5982–5991 (2019) [3](#)

# Supplementary File for ‘Multi-Task Label Discovery via Hierarchical Task Tokens for Partially Annotated Dense Predictions’

Jingdong Zhang<sup>\*</sup>, Hanrong Ye, Xin Li, Wenping Wang, Dan Xu

In this supplementary document, we present: (i) more details about the multi-scale global task token learning and task loss formation, (ii) more comprehensive explanation on experimental implementations, and (iii) more quantitative and qualitative experimental results.

## Appendix A Model Details

### Appendix A.1 Discrete Quantization and Task Losses

In Sec. 3 of the body part, we have discussed how to learn HiTTs. For continuous regression tasks, such as Depth and Normal, we first need to perform a discrete quantization of the label space to provide discriminative supervision for tokens. The goal for quantization is to assign meaningful category bins to each fine-grained token for classification. As analyzed in [2], this quantization only changes the way of predicting regression task, but does not contribute to the learning performance. For depth estimation, we follow the setting in [2, 16], and divide the range of depth values into several logarithmic bins. Our predicted task logits score  $\mathbf{G}'_i$  is used to calculate the soft-weighted sum with each bin and produce final task predictions accordingly. For surface normal estimation, we follow [2, 43] and use K-means to learn several unit normal vectors, which serve as clustering centers, and they are also used to generate predictions with  $\mathbf{G}'_i$ . This process can be expressed as:

$$\hat{\mathbf{Y}}_i = \text{Sum}(\mathbf{c}_i^\top \times \text{Softmax}(\mathbf{G}'_i)), \quad (10)$$

where  $\mathbf{c}_i \in \mathbb{R}^{C_p}$  represents the center of each bin. In our experiments, the numbers of depth bins and normal cluster centers on NYUD-v2 are 30 and 20, respectively. For Cityscapes, we consider 100 depth bins as the Cityscapes dataset is captured from outdoor scenarios and have more significant changes in depth. For PASCAL-Context, we select 40 different unit vectors uniformly from the space to serve as normal cluster centers.

To supervise the task predictions, we can directly impose regression losses on  $\hat{\mathbf{Y}}_i$  for Depth. and Normal:

$$L_i^{\text{reg}}(\hat{\mathbf{Y}}_i, \mathbf{Y}_i), \quad (11)$$

where  $L_i^{\text{reg}}(\cdot)$  can be  $L_1$  loss or Angle loss for Depth. or Normal. respectively. Furthermore, in order to gain more discriminative task category information for each token, we also impose classification loss on  $\mathbf{G}'_i$ . We first extract the corresponding one-hot label from  $\mathbf{Y}_i$  by  $\mathbf{c}_i$ , denoting as  $\mathbf{Y}_i^{\text{oh}}$ , and the loss can be written as:

$$L_i^{\text{cls}}(\mathbf{G}_i, \mathbf{Y}_i^{\text{oh}}) = -\mathbf{Y}_i^{\text{oh}} \cdot \log(\text{Softmax}(\mathbf{G}'_i)), \quad (12)$$

and the overall **mixture loss** for each task can be written as:

$$L_i(\cdot) = \lambda_i L_i^{\text{reg}}(\hat{\mathbf{Y}}_i, \mathbf{Y}_i) + L_i^{\text{cls}}(\mathbf{G}'_i, \mathbf{Y}_i^{\text{oh}}), \quad (13)$$

where  $\lambda_i = 0.1$  if task  $i$  is a regression task itself, otherwise  $\lambda_i = 0$ .

### Appendix A.2 Multi-scale Global Task Token Learning

For the implementations on NYUD-v2 and Cityscapes, we use the SegNet [1] to serve as the shared backbone, which produces single-scale shared features for per-task decoding. However, on PASCAL-Context, we use ResNet-18 [11] as the shared backbone, which can produce multi-scale shared features for decoding. Directly fusing them ignores the various task information maintained in different scales. Thus, we propose to learn the global task tokens on different scales in order to learn more comprehensive task relations.

As shown in Fig. 12, compared with the single-scale global task token learning process, the multi-scale process involves *inter-task learning* separately on each scale, and then the multi-scale features and tokens are fused before *intra-task learning*. The multi-scale backbone features  $\{\mathbf{F}_s^{(j)}\}, j = 0, 1, 2, 3$  are first flattened on each scale, and each global task token  $\theta_i$  is projected by a linear layer to produce multi-scale tokens:

$$\theta_i^{(j)} = \mathbf{W}_i^{s \rightarrow m^{(j)}} \times \theta_i, \quad j = 0, 1, 2, 3, \quad (14)$$

where  $\mathbf{W}_i^{s \rightarrow m^{(j)}}$  Then, for every feature  $\mathbf{F}_s^{(j)}$  and token  $\theta_i^{(j)}$  on scale  $j$  and task  $i$ , we query  $\mathbf{F}_s^{(j)}$  to obtain task features  $\{\mathbf{F}_i^{(j)}\}, i = 1, 2, \dots, T; j = 0, 1, 2, 3$ . After that, on each scale, we concatenate features and

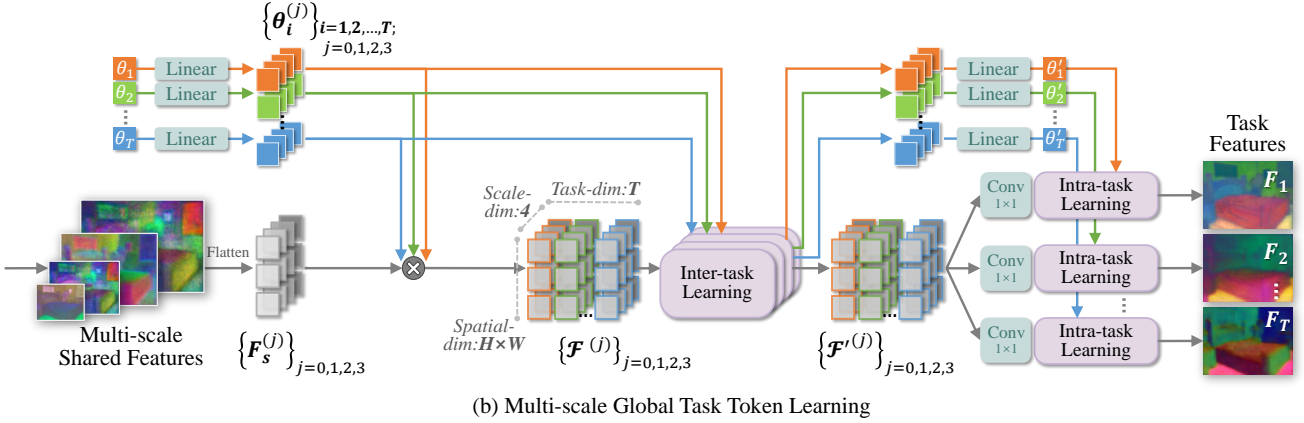
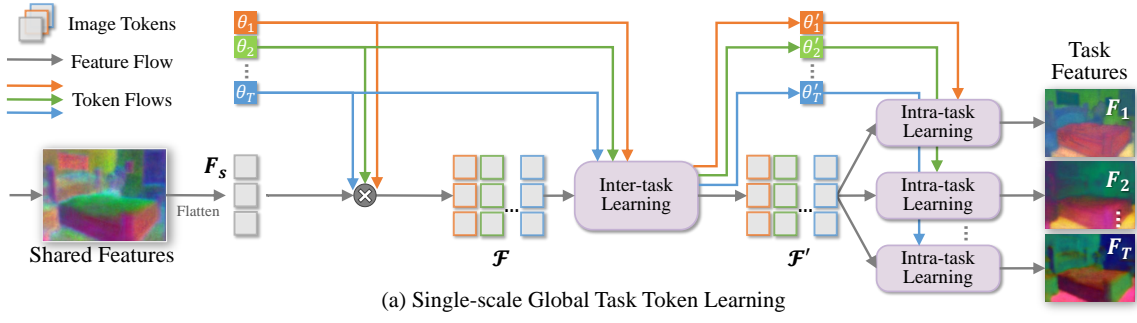


**Fig. 12** Illustrations of (a) *Single-scale* Global Task Token Learning and (b) *Multi-scale* Global Task Token Learning. For the multi-scale features produced by the shared backbone, we use linear layers to produce corresponding task tokens for each scale. Then, in each scale, we query task features and conduct inter-task learning to gain multi-task multi-scale representations. The multi-scale features and tokens are fused before intra-task learning to transfer cross-scale information.

tokens from every task for *Inter-task Learning* similar to Sec. 3.1:

$$\mathcal{F}^{(j)} = \left[ \mathbf{F}_1^{(j)}; \mathbf{F}_2^{(j)}; \dots; \mathbf{F}_T^{(j)} \right]^\top, \quad (15)$$

$$\Theta^{(j)} = \left[ \theta_1^{(j)}; \theta_2^{(j)}; \dots; \theta_T^{(j)} \right]^\top. \quad (16)$$

Subsequently,  $\mathcal{F}^{(j)}$  and  $\Theta^{(j)}$  are used for inter-task learning on each scale. We denote the features and tokens after intra-task learning as  $\mathcal{F}'^{(j)}$  and  $\Theta'^{(j)}$ . We fused them to share cross-task information on each scale:

$$\mathbf{F}'_i = \text{Conv}_i^{1 \times 1} \left( \left[ \mathbf{F}'_i^{(0)}; \mathbf{F}'_i^{(1)}; \mathbf{F}'_i^{(2)}; \mathbf{F}'_i^{(3)} \right] \right), \quad (17)$$

$$\theta'_i = \sum_{j=0}^3 \left( \mathbf{W}_i^{m \rightarrow s^{(j)}} \times \theta_i^{(j)} \right). \quad (18)$$

Finally, on each task  $i$ , the updated task features  $\mathbf{F}'_i$  and global task tokens  $\theta'_i$  are used for *Intra-task Learning*. The process is the same as Sec. 3.1.

In this way, we achieve learning global task tokens on multi-scale task features, which gains richer cross-task relations on different scales and maintains stronger representations in the global task tokens.

## Appendix B Implementation Details

**Model Setting.** We use SegNet [1] as the image backbone for our experiments on NYUD-v2 and Cityscapes; and we use ResNet-18 as the image backbone, Atrous Spatial Pyramid Pooling (ASPP) [3] as the task-specific decoding heads. For the threshold  $\tau_i$  which selects binary mask  $\mathbf{M}_i^P$ , we use {Semseg: 0.9, Depth: 0.45, Normal: 0.6} for NYUD-v2 one-label setting, {Semseg: 0.9, Depth: 0.7, Normal: 0.7} for NYUD-v2 random-labels setting, {Semseg: 0.9, Depth: 0.5} for Cityscapes one-label setting, and {Semseg: 0.9, Parsing: 0.85, Normal: 0.7, Sal: 0.7, Edge: 0.9} for PASCAL-Context one-label and random-labels settings.

## Appendix C More experimental results

### Appendix C.1 More Quantitative Results

**Analysis of Multi-Scale Global Task Token Learning.** As we illustrated in Sec. Appendix A.2, we adopt multi-scale global task learning with ResNet-18 backbone on PASCAL-Context. To validate the effectiveness of learning global task tokens on multi-scale fea-

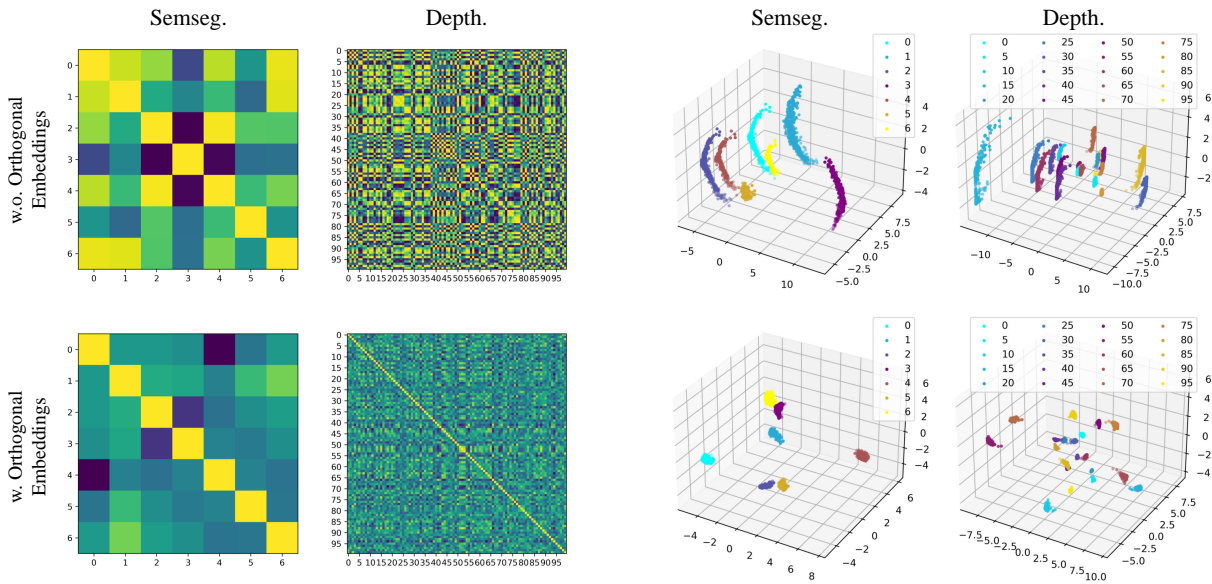


**Fig. 13** Visualization of self-affinities heatmap (*left*) and PCA for distributions (*right*) of fine-grained task tokens of the two tasks on Cityscapes validation set. With orthogonal embeddings, the affinities between different tokens are low and the clustering of token distributions on each category is better, which has a similar phenomenon to the visualization in Fig. 7 of the body part.

**Table 9** Comparison of HiTTs with *Single-scale* (SS) and *Multi-scale* (MS) Global Task Token Learning on PASCAL-Context under the *one-label* and *random-labels* setting.

Setting	Model	Semseg. <i>mIoU</i> ↑	Parsing. <i>mIoU</i> ↑	Norm. <i>mErr</i> ↓	Sal. <i>mIoU</i> ↑	Edge. <i>odsF</i> ↑	$\Delta_{MTL}$ (%)↑
One-Label	STL	47.7	56.2	16.0	61.9	64.0	-
	MTL <i>baseline</i>	48.4	55.1	16.0	61.6	66.5	0.59
	HiTTs (SS)	51.0	54.7	16.2	61.7	66.1	1.19
	HiTTs (MS)	52.3	56.2	15.8	62.0	67.9	3.43
Random-Labels	STL	60.9	55.3	14.7	64.8	66.8	-
	MTL <i>baseline</i>	58.4	55.3	16.0	63.9	67.8	-2.57
	HiTTs (SS)	59.1	53.4	15.0	64.1	67.8	-1.60
	HiTTs (MS)	60.3	55.3	14.7	64.6	70.2	0.76

tures, we compare the performance of Global Task Token Learning with single-scale and multi-scale backbone features respectively in Table 9. As shown in the table, HiTTs with single-scale (SS) Global Token Learning surpass the MTL *baseline* on both one-label and random-labels settings, with overall +0.60%  $\Delta_{MTL}$  and +0.97%  $\Delta_{MTL}$  on all tasks respectively, and the multi-scale (MS) Global Token Learning further enhances the performance to +2.84%  $\Delta_{MTL}$  and +3.33%  $\Delta_{MTL}$  on all tasks, which indicates the effectiveness of applying global token learning on multi-scale features.

## Appendix C.2 More Qualitative Results

We provide more qualitative results mainly from four parts: more visualization of the fine-grained token dis-

tributions, more comparisons of task score maps produced by HiTTs, more qualitative prediction comparisons, and the quality of generated pseudo labels.

**Visualization of token distributions.** We also provide visualization analysis to show the distributions of fine-grained task tokens on the two tasks of Cityscapes. In Fig. 13, with the aid of OE, the tokens are more orthogonal with each other as shown in the affinity maps, and have better clusters in the feature space as shown in the PCA distributions.

**Comparisons of Task Score Maps.** We visualize score maps produced by global task tokens and fine-grained task tokens respectively on each task. As shown in Fig. 14, we conduct visualization on both NYUD-v2 and Cityscapes datasets. The score maps indicate the response of task features to task tokens, and the

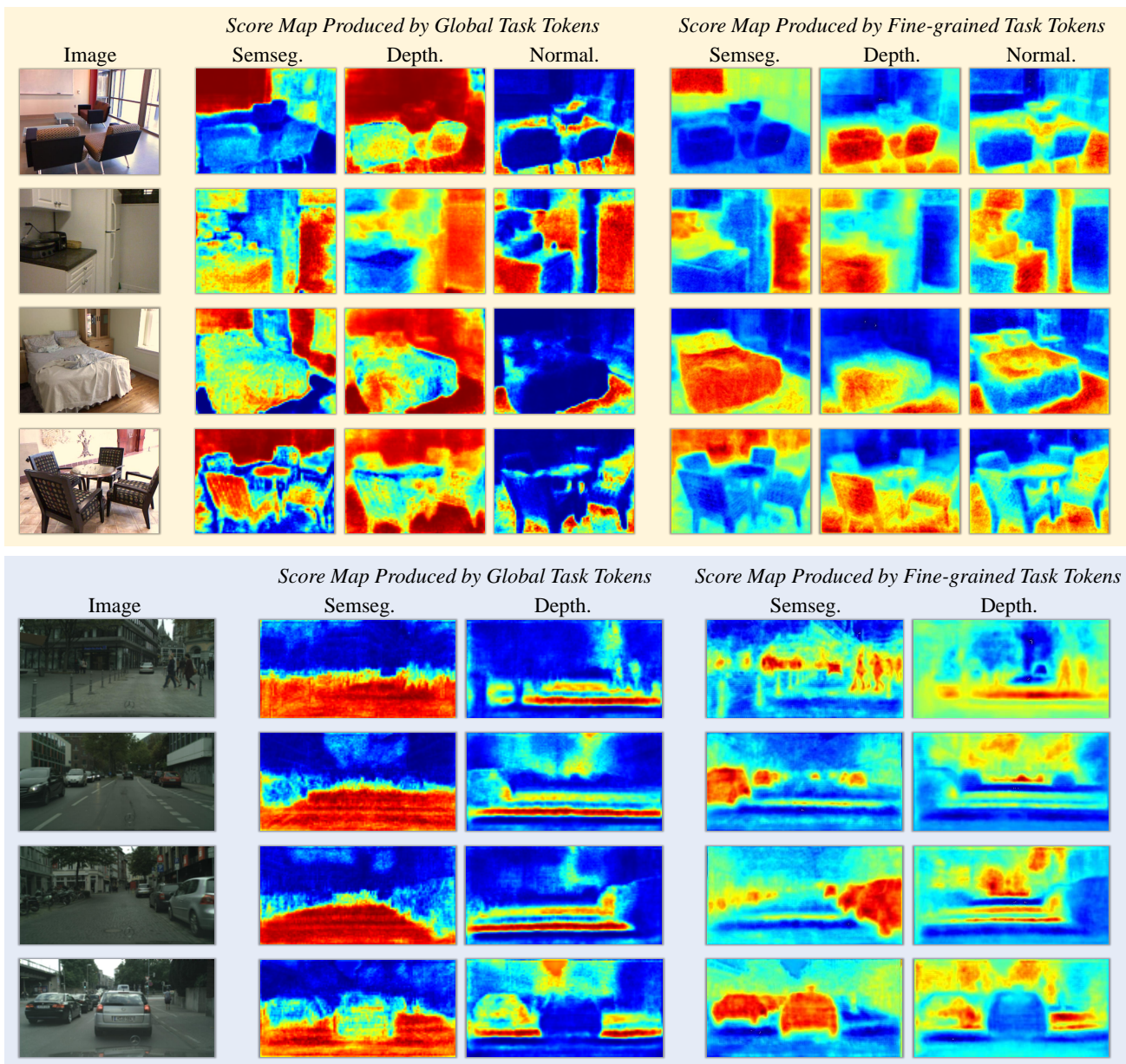


**Fig. 14** Comparisons of task score maps produced by global task tokens and fine-grained task tokens. The upper part is the visualization of samples on NYUD-v2 while the lower part is on Cityscapes. The score maps indicate the response of task features to task tokens, those produced by global task tokens are relatively noisy and monotonous, while those generated by fine-grained task tokens have finer granularity and less noise, which shows the hierarchy of the HiTTs learning process.

response patterns of feature maps on different tasks are very different, e.g. Semseg. features highlight areas with distinguish semantics, Depth. features focus on areas with a certain depth range and Normal. features focus on surfaces with the same orientation.

Comparing the score maps produced by tokens from different hierarchies, we find that score maps produced by global task tokens are relatively rough and noisy, while those generated by fine-grained task tokens have finer granularity and less noise, which shows the hi-

erarchy of the HiTTs learning process. Also, we observed that the high-light areas of global task tokens are monotonous, while fine-grained task tokens can high-light more details. This phenomenon is clearly observed in Cityscapes, since the ground truths of this dataset follow the long-tail distribution, thus the global task-tokens tend to learn the category with more pixel samples, and consequently always highlight the road area as shown in Fig. 14. However, the fine-grained tokens can give attention to more details, including the vehi-

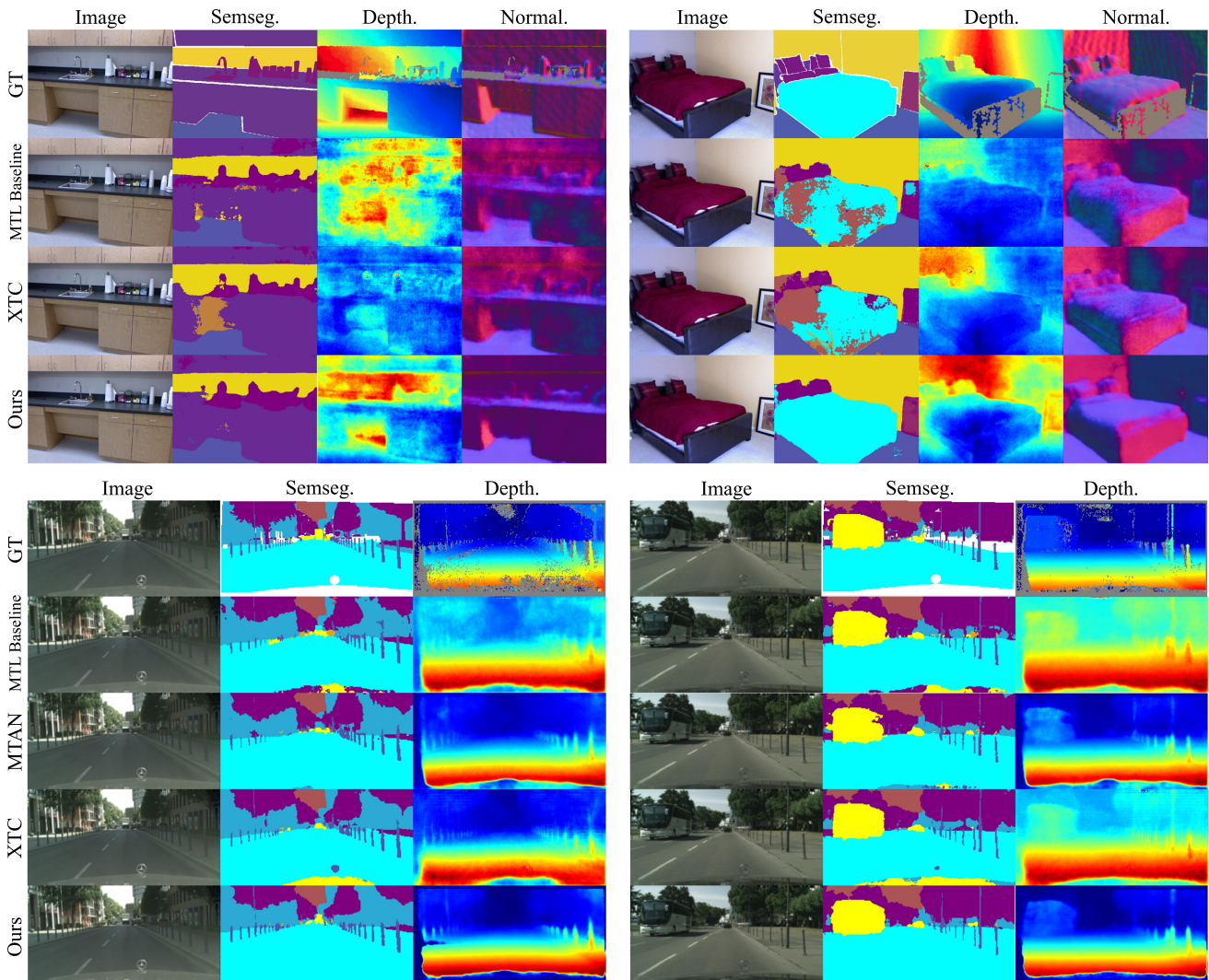


Fig. 15 Comparisons with SOTA works on NYUD-v2 (upper part) and Cityscapes (lower part).

cles and pedestrians with fewer pixel samples. Thus, it is necessary to design a hierarchical structure for tokens to learn representations with different granularity.

**Qualitative prediction comparisons with SOTA works.** We additionally provide comparisons with SOTA works on NYUD-v2 and Cityscapes. As shown in Fig. 15, we compare with MTL *baseline*, XTC [17] on NYUD-v2 three tasks, and with MTL *baseline*, MTAN [20], XTC [17] on Cityscapes two tasks. Our method shows clearly better performance in semantic understanding and accurate geometry estimations (including depth and normal estimation), indicating the effectiveness of our method.

**Visualization of Pseudo Labels.** In Fig. 16, we show pseudo task label maps generated by fine-grained task tokens. The pseudo label on different tasks has good quality without ground-truth supervision, which proves

the effective cross-task learning and strong generalization ability brought by HiTTs.

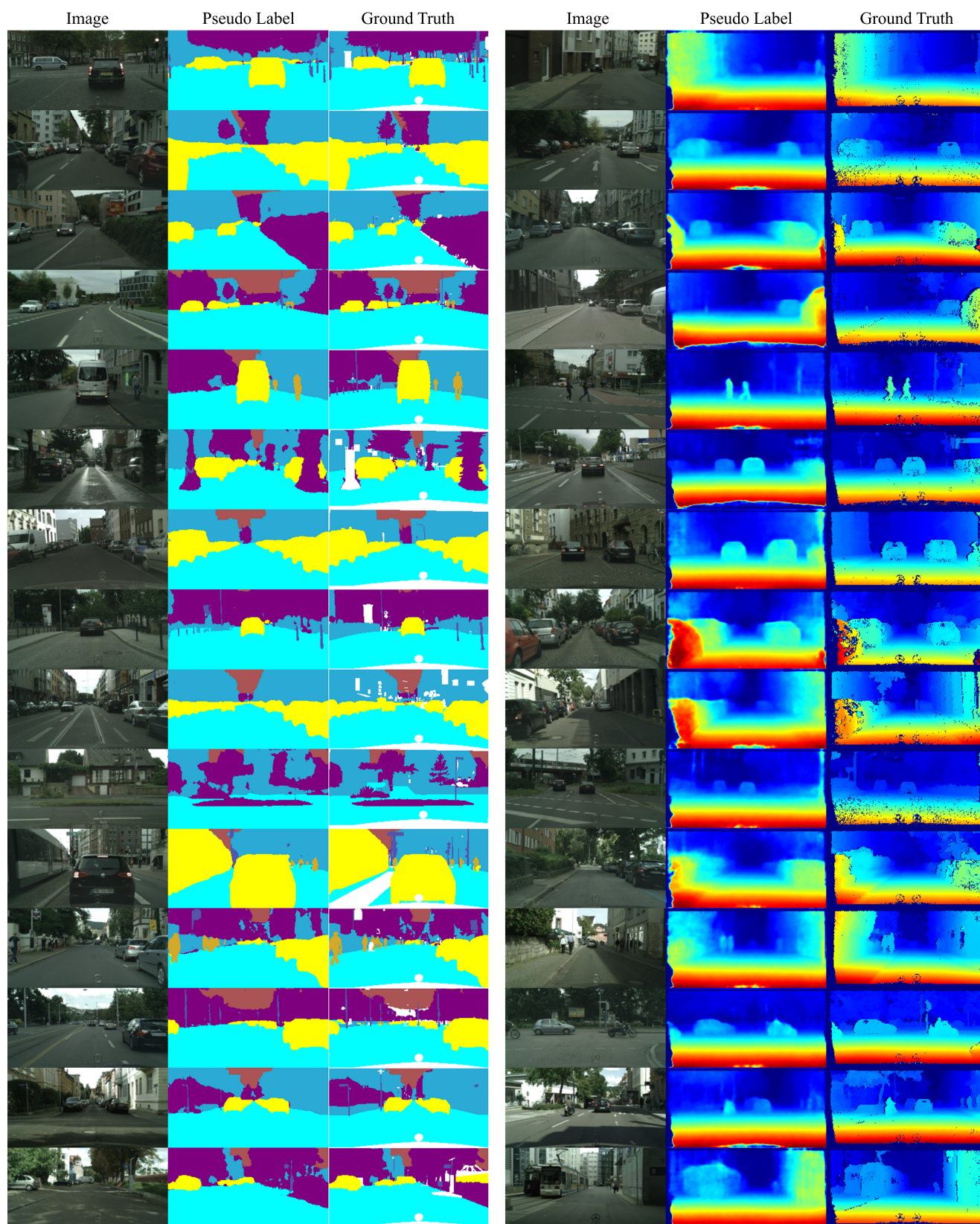


Fig. 16 Quantitative analysis of the quality of pseudo labels generated by global task tokens.